**Doctoral Dissertation**

博士論文

# Neural circuitry underlying backward escape behavior upon noxious light irradiation in *Drosophila* larvae

（ショウジョウバエ幼虫の後退行動を規定する神経基盤）

**A Dissertation Submitted for the Degree of Doctor of Philosophy**

**December 2019**

令和元年 12 月博士（理学）申請

**Department of Biological Sciences, Graduate school of Science,**

**The University of Tokyo**

東京大学大学院理学系研究科 生物科学専攻

**Natsuko Omamiuda-Ishikawa**

大豆生田(石川) 夏子

# Abstract

Animals typically avoid dangerous situations with stereotypic escape behavior. For instance, *Drosophila* larvae perceive intense blue light as noxious stimuli and respond with stereotypic escape behavior consisting of rapid forward locomotion, head-casting, rolling, or backward locomotion. Two sensory systems mediate the light-induced larval escape behavior redundantly: the photoreceptor-containing Bolwig's organ (BO) located on the head and the class IV dendritic arborization (C4da) neurons that tile the body wall. Either one of these sensory systems can evoke escape behavior, although the relationship between BO and C4da neurons at the neural circuit level remains elusive. Therefore, I asked how these two distinct sensory pathways can be integrated into a neural circuitry and evoke appropriate escape behavior.

First, to identify neurons that evoke a specific type of escape behavior, I conducted an optogenetic behavior screening in which particular subsets of neurons are optogenetically activated to analyze induced behavior. Consequently, I identified two sets of neurons that evoke robust backward locomotion, one type of escape behavior upon optogenetic activation. The first set is reported as the Moonwalker Descending Neurons (MDNs), whose activation induces backward locomotion. The other set of neurons evoked similar behavior to the one induced by MDN activation, although it was composed of a different subset of novel neurons. I named this novel subset of neurons the Ascending Moonwalker-like Backward neurons (AMBs).

To further characterize MDNs and AMBs, I determined the transmitter identity and the morphology of each neuron. I found that AMBs were choline acetyltransferase (ChAT) positive neurons using immunofluorescence, suggesting that they are cholinergic neurons. From the morphological analysis, I found that MDNs were composed of two pairs of descending neurons, while AMBs were composed of one pair of ascending neurons.

Considering the observation that activation of either AMBs or MDNs triggers similar backward locomotion, I hypothesized that AMBs and MDNs might function in the same neuronal circuits. To test this possibility, I analyzed the relationship between AMBs and MDNs morphologically and functionally. First, I dual-labeled AMBs and MDNs and found that AMB axons were closely apposed to MDN dendrites, implying that AMBs are presynaptic to MDNs. This was directly confirmed by the GFP Reconstitution Across Synaptic Partners (GRASP) analysis between MDNs and AMBs, in which the GRASP signals were located at the presynaptic terminal of AMBs. The synaptic connection between AMBs and MDNs was further validated by functional analysis using $Ca^{2+}$ imaging and optogenetics. Finally, behavioral analysis indicated that AMBs function upstream of MDNs. Although activation of AMBs induced repetitive backward waves in the control experiment, silencing of MDNs by tetanus toxin (TNT) significantly reduced this behavior. Taken together with my morphological and functional analyses, I conclude that AMBs function presynaptically to MDNs to evoke backward locomotion.

The results obtained so far indicate that the AMB-MDN pathway induces backward locomotion, however, upstream of the pathway still remains elusive. Thus, I asked which sensory pathways might be mediated by the AMB-MDN pathway using an optogenetic behavior assay and $Ca^{2+}$ imaging. I first showed that MDN silencing inhibited backward waves induced by BO and C4da neurons, while AMB silencing inhibited backward waves induced by C4da neurons but not by BO. I next showed that optogenetic activation of C4da neurons, but not BO, resulted in a significant increase of $Ca^{2+}$ signal in AMBs. I further tested whether AMBs indeed relay physiological blue light information from the C4da pathway or not by $Ca^{2+}$ imaging. I found that control larvae showed a significant increase of $Ca^{2+}$ signal in AMB somas in response to blue light irradiation while C4da-ablated larvae did not. Taken all the data together, I concluded that the AMB-MDN pathway mediates noxious blue light signals from C4da sensory neurons to evoke backward locomotion.

In summary, my study revealed a local neural circuit that mediates backward locomotion induced by noxious information. My data indicate that AMBs, which are newly identified backward neurons in this study, are direct presynaptic partners of MDNs, command-like neurons for backward locomotion induced by noxious light. AMBs are essential for C4da-induced backward waves but are not required for BO-induced backward waves. Based on the following lines of evidence, I propose that MDNs would work as convergence points for distinct sensory inputs to integrate signals in order to trigger backward locomotion. First, AMBs are direct presynaptic partners of MDNs. Second, AMBs are not required for BO-induced backward waves. Third, MDNs are required for backward locomotion induced by noxious light, which is mediated by BO and C4da neurons redundantly. My findings could further contribute to the elucidation of the circuit-based mechanism of how multiple sensory inputs are integrated to regulate specific behavior.

# Table of contents

# Abbreviations

| | |
|---|---|
| ATR | All-trans retinal |
| AMB | Ascending Moonwalker-like Backward neuron |
| BO | Bolwig's organ |
| ChAT | Choline acetyltransferase |
| C3da neuron | Class III dendritic arborization neuron |
| C4da neuron | Class IV dendritic arborization neuron |
| CNS | Central nerve system |
| GABA | Gamma Aminobutyric Acid |
| GRASP | GFP reconstitution across synaptic partners |
| LC16 neurons | Lobula columnar 16 neurons |
| MDN | Moonwalker Descending neuron |
| PBS | Phosphate-Buffered Saline |
| ROI | Region of interest |
| SEZ | Subesophageal zone |
| TEM | Transmission electron microscopy |
| TLA neurons | TwoLumps Ascending neurons |
| TNT | Tetanus neurotoxin light chain |
| UAS | Upstream activating sequence |
| VGluT | Vesicular glutamate transporter |
| VNC | Ventral nerve cord |

# Introduction

Locomotion is an evolutionally conserved motor function. Most animals can move not only in the forward direction but also in other directions. For example, legged vertebrates use the spinal network to walk in any direction [1,2]. Even if the animals do not have legs, they have their way of changing the direction of locomotion. Lower vertebrates such as lamprey or zebrafish can swim backward [3,4]. Invertebrates such as nematodes or fly larvae can crawl backward [5,6]. The change in the direction of locomotion is usually generated in the context of avoidance behavior and is critical for animals to avoid danger [7–9]. Among various types of locomotion changes, the selection between forward and backward locomotion is especially important to avoid injury or predation since forward, and backward locomotion is mutually exclusive. Thus, animals often have dedicated neural systems for backward locomotion [5,10]. In the vertebrates, the spinal network and supraspinal commands determine the direction of locomotion specifically for each direction. The mesencephalic locomotor region has been reported as a command center of forward locomotion [11,12]. However, the existence of command centers for other directions such as sidewalks or backward remains unknown. In the invertebrate's model system, *Caenorhabditis elegans* has dedicated motor neurons and command-like neurons for forward and backward locomotion [5,13–15]. Command-like neurons are small subsets of neurons whose activation results in the initiation of a specific physiological behavior [8,16,17]. Using a relatively simple model with tractable neural circuits, previous studies have revealed neural mechanisms underlying the control of the locomotion direction [18,19]. However, it remains unclear how other organisms having more complex nervous systems, such as insects and mammals, could control locomotion directions. Here I use the model animal, *Drosophila melanogaster*, to tackle this issue. The *Drosophila* nervous system is relatively complex, consisting of 10,000–15,000 neurons [20], and produces stereotyped locomotor behavior repertoires, including forward locomotion, bending, and backward locomotion. Importantly, sophisticated genetic tools to manipulate specific cell types such as the GAL4/UAS binary expression system, the LexA/LexAop

system as well as the thousands of the GAL4 or the LexA line collections, are available for the *Drosophila* research [21,22], allowing the expression of transgenes that enable manipulation of neuronal activity in genetically-defined subsets of neurons.

A recent study reported that *Drosophila* larvae also have backward and forward specific neural systems as vertebrates or nematodes have [23]. As a descending control for backward locomotion, *Drosophila* utilizes the command-like Moonwalker Descending Neurons (MDNs) that are two pairs of descending cholinergic neurons in the brain [6,24]. MDNs keep the role of regulating backward locomotion from the larval stage to the adult stage [6]. Structural studies utilizing transmission electron microscopy (TEM) and functional studies utilizing a calcium indicator showed that MDNs promote backward locomotion in response to mechanical stimuli, presumably through activating the backward-specific premotor neurons and simultaneously suppressing forward premotor neurons through distinct postsynaptic partners in the larval stage such as ThDN, A18b, and Pair1 [6].

Although a previous study focused on the motor circuits located downstream of larval MDNs [6], sensory control of backward locomotion in the larval stage remains unclear. The study reported that MDNs have 396 upstream synaptic inputs per cell on average, but it failed to detect mono-synaptic sensory input into MDNs in the larval stage [6]. In the adult stage, two sets of upstream neurons have been reported: the lobula columnar 16 (LC16) neurons and the TwoLumps Ascending (TLA) neurons, which convey visual inputs from photoreceptor cells and touch inputs from legs, respectively [25,26]. However, there has been no report on the upstream neurons sending synaptic inputs to the larval MDNs.

Some sensory circuits are assumed to be located upstream of MDNs to induce backward locomotion in response to sensory stimuli. Previous studies reported that several types of stimuli could induce backward locomotion in *Drosophila*. One is mechanosensory stimuli, which are achieved by a "dead-end" in the adults [24,25] or a head-poke in the larvae [6,27]. The other is visual stimuli, which are achieved by looming visual stimuli in the adults [28] or blue light irradiation on the anterior part of the body in the larvae [27,29].

The mechanical response of Drosophila larvae depends on two types of sensory neurons: the class III dendritic arborization (C3da) neurons and the class IV dendritic arborization (C4da) neurons (Fig. 1) [30]. Both C3da and C4da neurons cover the entire body wall of larvae and project to the ventral nerve cord (VNC). The two sensory neurons express different mechanotransduction channels so that they receive different amplitudes of mechanical stimuli. C3da neurons express the mechanotransduction channel *No mechanoreceptor potential C* (*NompC*) to sense gentle touch [30], whereas C4da neurons express *Piezo* and *pickpocket* (*ppk*) to sense noxious mechanical stimuli but not gentle touch [31]. Previous studies on the larval MDN utilized a head-poke conducted by both harsh touch and gentle touch [6,27]. Thus, it is possible that either C4da or C3da pathways are upstream of MDNs. Consistent with this idea, a recent study has identified a subset of neurons in the VNC, Wave neurons, which are secondary neurons of C3da and C4da sensory neurons to induce segment-specific escape behavior including forward or backward locomotion [27]. However, this study showed that the Wave circuit sufficiently induced backward locomotion even without a connection between the VNC and the brain [27]. This result indicates that Wave neurons can induce backward locomotion within a neural circuit in the VNC and that Wave neurons do not necessarily connect to MDNs functionally to induce backward locomotion. Hence, little is known about the upstream circuits that convey signals to MDNs for backward locomotion upon mechanical stimulation.

The visual response of *Drosophila* larvae depends on two partially redundant sensory systems, the Bolwig's organ (BO) and the C4da neurons (Fig. 1) [29]. The BO is a pair of a cluster of photoreceptors located on the larval head and project to the brain [32,33]. Similar to the mechanosensory system, the two sensory neurons use a different molecular mechanism to sense light having different wavelengths. The BO expresses two types of rhodopsin, *Rhodopsin 5* (Rh5) and *Rhodopsin 6* (Rh6), which sense blue and green, respectively [32]. The C4da neurons express two isoforms of *dTRPA1* and sense photochemical $H_2O_2$ production by strong UV or blue light irradiation [34]. The ablation of either BO or C4da neurons attenuates light responses toward blue light

irradiation, and the effects are additive [29]. Although recent studies have identified several neurons that are downstream of C4da sensory neurons to evoke rolling behavior [27,35–38] or BO to control light avoidance [32,39–42], their downstream circuits that control backward locomotion remain to be elucidated. Furthermore, although their contributions to light-sensing are additive, it remains mostly unknown how BO and C4da sensory circuits are integrated to evoke escape behavior upon light irradiation [29].

In the present thesis, I identified a pair of neurons in the subesophageal zone (SEZ), designated as the Ascending Moonwalker-like Backward neurons (AMBs), which induce repetitive backward locomotion through a non-biased optogenetic screening. My structural and functional analyses showed that AMBs are presynaptic to MDNs and send excitatory signals to MDNs to elicit backward locomotion. Further behavioral and functional analyses revealed that AMBs specifically relay noxious information from C4da neurons, but not from BO to MDNs in order to trigger backward locomotion. My present thesis thus uncovered neural circuit mechanisms in which two distinct sensory pathways for noxious stimuli are integrated to evoke specific escape behavior.

# Materials and methods

### Fly stock and Transgenic Flies

I used both male and female early third instar larvae (after egg laying 72-96 h) of *Drosophila melanogaster* in all experiments. I raised larvae on the standard medium at 25°C in the total dark condition unless otherwise specified. I obtained fly stocks carrying $w^{1118}$ (BL#3605), tub-$GAL80^{ts}$ [43] (BL#7017), tub-FRT-GAL80-FRT (BL#38880), UAS-TNT(BL#28838), UAS-CsChrimson::mVenus (BL#55135, BL#55136), R27H06-LexA (BL#54751), VGlut-GAL80[MI04979] (BL#60316), R60F09-GAL4 (BL#39255), R60F09-LexA (BL#61576), R73D06-GAL4 (BL#46692), R73F04-GAL4 (BL#49623), R60F09-GAL4DBD (BL#75644), R11E07-p65AD (BL#68816), UAS-mCD8GFP (BL#5137), UAS-GCaMP6m (BL#42748), LexAop-CsChrimson::mVenus (BL#82183), LexAop-GAL80 (BL#32215), LexAop-GCaMP6m(BL#44276), LexAop-GCaMP6s (BL#44590), UAS-mCD8RFP (BL#32229), LexAopmCD8GFP (BL#32229), GMR-GAL4 (BL#1104), ppk-GAL4 (BL#32079), NompC-GAL4 (BL#36369), UAS-post-t-GRASP and LexAop-pre-t-GRASP (BL#79039) and UAS-DenMark (BL#33061) from Bloomington Drosophila Stock Center. Otd-FLPo by David Anderson (California Institute of Technology); tsh-GAL80 by Gero Miesenböck (University of Oxford); LexAop-rCD2RFP by Tzumin Lee (Janelia Research Campus); UAS-BrpD3::mCherry by Takashi Suzuki (Tokyo Institute of Technology); SS01613-GAL4 by Chris Doe (University of Oregon); 19-12-GAL4 and repo-GAL80 by Jay Parrish (University of Washington); UAS-rpr, UAS-hid by Douglas Allan (University of British Columbia). R73F04-LexA by cloning R73F04 from the genome of $w^{1118}$ using the primers described in FlyLight (http://flweb.janelia.org/) into pENTR 1A vector (Thermo Fisher Scientific, A10462) and subsequently exchanged to pBPnlsLexA::p65Uw (Addgene, #26230) according to the previously described method [21]. I generated Gad1-2A-GAL80 using the CRISPR/Cas9 system as described in the previous studies [44,45]. I inserted transgene encoding the 2A peptide and the *GAL80* gene in front of the stop codon of the *Gad1* gene with the following 20-bp guide RNA (gRNA) sequence: 5′-

GCCTGGGCGACGACTTGTAA-3′. The engineered locus encodes a bicistronic transcript that produces Gad1 and GAL80 proteins, thereby allowing me to express GAL80 in the same spatiotemporal pattern as the endogenous Gad1 protein.

**The optogenetic screening**

In order to systematically identify any neurons that, upon activation, would show a specific type of escape behavior, I designed an unbiased optogenetic screening in the third-instar *Drosophila* larvae. This screening used the Janelia collection of GAL4 lines [22] and UAS-CsChrimson [46] transgenes to express light-gated cation channels in arbitrary neurons. In addition, I used tsh-GAL80 [47,48] that is a transgene to induce GAL80, which is a suppressor of GAL4 activity, in the VNC in order to specify the expression of CsChrimson in the neurons locating in the brain or the SEZ because the VNC include the somas of motor neurons whose activation can mask the behavioral effect of other neurons' activation. I crossed 5 male flies of GAL4 lines with 20 female flies harboring UAS-CsChrimson and tsh-GAL80 transgenes and then collected the eggs for 24 hours. The larvae grew in the standard medium containing 0.5 mM all-trans retinal (ATR; Sigma Aldrich, #R2500) at 25°C. I floated larvae using 20% sucrose, and then gently washed by distilled water to collect them on an agarose plate. The behavioral experiment was conducted on a 1% agarose gel plate in φ 9 cm plastic dish. I placed 15 larvae on the center of the plate at one trial. I repeated three trials for each genotype. For optogenetic activation, I applied 617 nm light (Thorlabs, M617L4, 34.0 $\mu W/mm^2$) for 5 minutes. I recorded the larval behavior with CCD Camera (Thorlabs, 1500M-GE) for 1 fps with the infrared background illumination (CCS, LDR2-132IR940-LA), and classified its behavior phenotype manually.

**Immunohistochemistry**

I dissected early third instar larvae in phosphate-buffered saline (PBS) and fixed them in 4% paraformaldehyde/PBS for 15 minutes at room temperature. For imaging without staining (Figs. 2-5, 8, and 16), I moved the larval CNS into 0.3 % Triton X-100/PBS (PBT) and incubated for 3 hours at

4°C after fixation. Then I moved the samples in VECTASHIELD mounting medium (Vector Laboratories, H-1000) to incubate for 3 hours, and imaged with confocal microscopy (Leica TCS SP8). For imaging with immunohistochemistry (Figs. 6 and 9), I moved the samples into PBT to incubate for 30 minutes after fixation. I blocked them for 30 minutes in PBT containing 5% normal goat serum (NGS) at 4°C on a shaker. I subsequently incubated the samples with a primary antibody diluted in 5% NGS/PBT at 4°C overnight. After washing the samples with PBT 5 times for 10 minutes each, I blocked them for 30 minutes in 5% NGS/PBT. I subsequently incubated the samples with a secondary antibody diluted in 5% NGS/PBT at 4°C overnight. After washing the samples with PBT 5 times for 10 minutes each, I transferred the stained samples into VECTASHIELD to incubate for 3 hours at 4°C and imaged with confocal microscopy. The antibodies used in this study and the dilutions are as follows: anti-ChAT (mouse monoclonal; hybridoma bank 4B1; 1:50), anti-GABA (rabbit polyclonal; Sigma Aldrich #110M4781; 1:100), anti-VGluT (rabbit polyclonal; a gift from Hermann Aberle [49]; 2-DVl-lut-N-TRIM (N); 1:400), anti-mouse Alexa Fluor 635 (goat IgG; Molecular Probes, #A31575; 1:500), anti-rabbit Alexa Fluor 633 (goat IgG; Molecular Probes, #A21071; 1:500), anti-HA (1:50; rat monoclonal; 3F10; Roche, 11 867 423 001) and anti-rat Cy5 (1:500; goat IgG; Molecular Probes, #A31575).

**Optogenetics in free-moving larvae**

The larvae grew in the standard medium containing 0.5 mM ATR at 25°C. I floated larvae using 20% sucrose, and then gently washed to collect them on an agarose plate. The behavioral experiment was conducted on a 1% agarose S gel plate (Wako, #13-90231) in φ9 cm plastic dish. I placed one larva on the center of the plate at one trial. For optogenetic activation, I applied 30 seconds of 640 nm light (Lumencor Spectra X7, 2.84 μW/mm$^2$ for Figs. 11A-11G or 93.3 μW/mm$^2$ for Figs. 3, 4, 11H-11I and 17) for CsChrimson activation. I recorded the larval behavior with sCMOS-Camera (Andor, Zyla 5.5) for 1 minute at 20 fps under a stereomicroscope (Olympus, MVX10) with the infrared background illumination (CCS, LDR2-132IR850-LA).

**Blue light assay**

The larvae grew in the standard medium at 25°C. I prepared the larvae and equipment in the same way as described in the optogenetics assay above. For stimulation, I applied a 440 nm spotlight (φ0.5 cm, 245 μW/mm$^2$, Lumencor Spectra X7) to the larvae on the agarose plate for five seconds. I targeted the light application to the anterior half of the larval body to induce backward locomotion. If the light did not cover the anterior half of the body, I excluded the trial from the analysis to minimize the variance of the stimulation. I performed one trial for each animal.

**Dead-end assay**

I prepared the larvae and equipment in the same way as described in the blue light assay above. I cut a pipette tip for 200 μl (WATSON) into 1 cm long from its pointed end and fused its terminal by heat to make a "dead-end" tube. I let the animal into the tube and waited until it voluntarily reached the dead-end. I started recording for 1 minute from their arrival at the dead-end. When the larva failed to reach the dead-end within 1 minute from the entry to the tip, I excluded the trial from the analysis. I performed one trial for each animal.

**Gentle touch assay**

I prepared the larvae and equipment in the same way as described in the blue light assay above. As a stimulus, I used an eyelash hair that has been glued to the end of a pipette tip, which could apply a force in the range of 1–10 μN [50]. I stroked the animal four times with intervals of 10-15 seconds in 1 minute for one trial. I performed one trial for each animal.

**Behavioral Analysis**

I quantified larval backward waves manually. I counted larval waves when larvae showed a sequence of muscle contractions across segments with the direction from anterior to posterior (backward) or posterior to anterior (forward). I counted rolling events when larvae showed more than one complete rotation toward the lateral side. For Figs. 3, 4, and 11A-11G, I analyzed 10 seconds

before or after the optogenetic stimulation onset. For Figs. 11H-1I and 17, I analyzed the entire 30 seconds of stimulation periods. For Fig. 12, I analyzed the whole recording period to count the number of backward waves. For Fig. 13, I analyzed larval behavior from the first frame of applying a stroke to the last frame for each trial. For Fig. 14, I analyzed 10 seconds after the onset of the blue light delivery. I counted larvae as "respond to blue light using backward waves" only when larvae do not show forward waves between the onset of light and the timing of backward waves. For Figs. 7, 11, and 15, I utilized FIMTrack [51] to track larval behavior. I picked up "go state", "bending state", and "coiled state" among the parameters calculated by the software. I defined "forward run" as the state in which "go state" is on and backward waves have not occurred, "bend" as the state where either right or left "bending state" is on, and "stop" as the state where neither "go state" nor "bending stop" is on. I excluded timeframes measured as a coiled state because FIMTrack fails to extract the posture correctly in coiled animals.

**Calcium Imaging**

I grew the larvae in the standard medium containing 0.5 mM ATR. The third instar larvae were pinned down on a silicon dish (Silpot 184, Dow Corning Toray) and dissected along the dorsal midline in the calcium-free HL3.1 buffer (NaCl 70 mM, KCl 5 mM, MgCl2 4 mM, NaHCO3 10 mM, Trehalose 5 mM, Sucrose 115 mM, HEPES 5mM, pH 7.2 [52]). I removed the internal organs except for neural tissues. I imaged the CNS using an Olympus BX51WI microscope equipped with a spinning-disk confocal unit CSU10 (Yokogawa) and an EM-CCD digital camera (Evolve, Photometrics). For the activation of neurons expressing CsChrimson, I applied 615 nm light (105 μW/mm2) with pE-100 (CoolLED). For the activation of blue light-sensitive neurons physiologically, I applied 475 nm light (208 μW/mm2) with a pE-300$^{ultra}$ device (CoolLED).

I quantified calcium probe signals using Fiji (Fiji is just ImageJ) and R (ver 3.2.2). I set regions of interest (ROI) on the neurites of MDNs or the somas of AMBs and calculated mean signal intensity within each ROI using Fiji. I got the raw signal intensity F and calculated F0 as the mean fluorescent

signals from 0 to 10 seconds before the optogenetic stimulation, and treated as a baseline. Then I calculated the normalized calcium transient in each ROI according to the formula $\Delta F/F = (F - F0) / F0$ using R. I calculated the mean of $\Delta F/F$ in 10 seconds after (ON) or before (OFF) the onset of the optogenetic stimulation and showed as the mean $\Delta F/F$ in ON or OFF state (Figs. 10 and 18). For Fig. 19, I calculated the mean of $\Delta F/F$ in 5 seconds before (OFF) or the last 5 seconds during (ON) optogenetic activation and showed as the mean $\Delta F/F$ in ON or OFF state.

**Statistical analysis**

I evaluated statistical significance using the Wilcoxon rank-sum test (Figs. 3-4 and 11-13), Fisher's exact test (Figs. 4H, 14, and 17), or Welch's two-sample t-test (Figs. 10, 18, and 19). I used the Holm method for multiple testing. "n" indicates the number of animals. Asterisks denote statistical significance: *** $p < 0.001$; ** $p < 0.01$; * $p < 0.05$; n.s., not significant ($p \geq 0.05$). All of the statistical analyses were performed by R version 3.3.2. I did not use any methods to determine whether the data met assumptions of the statistical approach.

# Results

### The optogenetic screening identified neural subsets which induce robust backward locomotion

In order to systematically identify neurons involved in the control of a specific type of escape behavior, I conducted an optogenetic screening in the *Drosophila* third instar larvae using the Janelia GAL4 collection and UAS-CsChrimson [22,46]. I chose 783 GAL4 lines that label less than 40 neurons in the brain, covering whole larval CNS consisting of 15,000 neurons on average when assuming that even a half of labeled neural subsets were overlapped. From the 783 GAL4 lines screened, I identified eleven GAL4 lines whose activation triggered robust backward locomotion. I focused on three GAL4 lines among them as it was challenging to subdivide the labeled population for further analysis in other GAL4 lines. I first checked whether these GAL4 lines could label MDNs because MDNs are known to trigger backward locomotion upon activation [6]. I found that one of the three GAL4 lines, R73F04-GAL4, appeared to label MDNs based on the cell morphology. Indeed, two pairs of descending neurons in R73F04-LexA are colabeled with RFP expression in MDNs using SS01613-GAL4, confirming that the two pairs of descending neurons labeled by R73F04-GAL4 are identical to MDNs [6] (Fig. 2).

### A single pair of ascending cholinergic neurons in SEZ can trigger backward locomotion

Since the other two GAL4 lines, R60F09-GAL4 and R73D06-GAL4, were unlikely to label MDNs, I attempted to genetically define the responsible neurons by combinatory expressions of a variety of GAL80 and FLP drivers together with R60F09-GAL4 [53,54]. Using these approaches, I subdivided R60F09-GAL4-positive neurons into distinct populations (Fig. 3, see Table. 1 for genotypes of GAL4). I found that optogenetic activation of the R60F09-ACh-GAL4 population, but not the R60F09-Brain-GAL4 population, significantly increased the number of backward waves (Figs. 3E and 3F). Since a pair of neurons in the subesophageal zone (SEZ) was observed in the R60F09-ACh-GAL4 population, but not in the R60F09-Brain-GAL4 population (Figs. 3B and 3C;

arrowheads), I focused my later studies on these neurons as potential candidates to induce backward locomotion and designated these neurons as the Ascending Moonwalker-like Backward neurons (AMBs).

**Validation of AMB-labeling lines**

To further examine whether AMBs are responsible for backward locomotion, I checked whether AMBs might be labeled by R60F09-LexA or R73D06-GAL4 as well as R60F09-GAL4. Imaging and optogenetic activation assay indicated that R60F09-LexA labeled fewer neurons than R60F09-GAL4 did but still labeled AMBs to induce backward locomotion upon activation (Figs. 4A-4C). Dual labeling with R60F09-LexA and R73D06-GAL4 indicated that AMBs in the SEZ are the only cells co-expressing both drivers in the larval CNS (Fig. 4D). Taking advantage of this restricted intersection, I tested the contribution of AMBs to backward locomotion induced by optogenetic stimulation of R73D06-GAL4-expressing cells. I found that larvae expressing LexAop-GAL80 with R60F09-LexA in addition to UAS-CsChrimson with R73D06-GAL4 did not show CsChrimson expression in AMBs (Fig. 4E). In these animals, there was a significant decrease in the number of the backward waves induced by R73D06-GAL4-expressing cells compared with larvae not expressing GAL80 in R60F09-LexA-expressing cells (Figs. 4F and 4G), further indicating that AMBs, which are the only neurons commonly activated in the two drivers, are indeed the responsible neurons to trigger backward locomotion. In addition to backward locomotion, optogenetic activation of R73D06-GAL4 neurons evoked rolling behavior (Fig. 4H). Unlike backward locomotion, rolling behavior was unaffected by R60F09>GAL80 (Fig. 4H), suggesting that rolling behavior evoked by optogenetic activation of R73D06-GAL4 neurons is mediated by other neurons rather than AMBs. Finally, I generated a splitGAL4 by combining R60F09-GAL4DBD and R11E07-p65AD, and confirmed that the split-GAL4 specifically labeled AMBs in the larval brain (Fig 3D) (hereafter, designated as AMB-GAL4). Optogenetic stimulation of AMB-GAL4-expressing cells induced significant backward locomotion (Figs 3E-3F). Taken together, I conclude that AMBs trigger backward

locomotion upon optogenetic activation.

Importantly, non-AMB populations in the neurons labeled by these transgenes do not induce backward locomotion (Fig. 3B, R60F09-Brain; Fig. 4E, R73D06>CsChrimson, R60F09>GAL80). It indicates that functional analysis using R60F09 or R73D06 is mostly attributed to the effect of AMB manipulation when the analysis focus on backward locomotion.

**Axon projection and transmitter characterization of AMBs**

I identified the novel backward-inducing neurons AMBs and developed ways to manipulate them so far. In the next step, I conducted anatomical analysis on AMBs to set up a hypothesis on how they work to induce backward locomotion. To locate dendrites and axons of AMBs, I expressed a dendritic marker Denmark [55] and a presynaptic marker BrpD3::mCherry [56]. Denmark labeled the somas and neurites from the SEZ to the T2 segment whereas BrpD3::mCherry localized in the neurites projecting to the brain (Figs. 5A and 5B), indicating that AMBs are ascending neurons that have dendritic arborizations in the SEZ to the T2 segment and extend axonal projections to the brain (Fig. 5E). I also characterized MDNs in the same way and found that Denmark labeled the somas and neurites in the brain, whereas BrpD3::mCherry localized in the neurites projecting to the VNC (Figs. 5C and 5D). This indicates that MDNs are descending neurons, which is consistent with the previous study [6]. I further analyzed the neurotransmitter of AMBs by immunostaining with antibodies against three transmitter markers [57], and found that AMBs were immunoreactive to the choline acetyltransferase (ChAT), but not to the vesicular glutamate transporter (VGluT) or GABA, indicating that AMBs are cholinergic neurons (Fig. 6A-6C). As a negative control, I confirmed that the samples without anti-ChAT did not show any fluorescent signal in AMBs (Fig. 6D). As a positive control, I confirmed that MDNs were ChAT positive as previously reported [6] (Fig. 6E).

**AMBs are anatomically presynaptic to MDNs**

Since activation of either AMBs or MDNs triggers similar backward locomotion (Fig. 7), I

reasoned that AMBs and MDNs might function in the same neuronal circuits. To test this possibility, I dual-labeled AMBs and MDNs using the GAL4/UAS and the LexA/LexAop binary expression systems and found that AMB axons were closely apposed to MDN dendrites in the brain (Fig. 8), implying that AMBs are presynaptic to MDNs. To further confirm that, I monitored synaptic GRASP (GFP reconstitution across synaptic partners) signal using t-GRASP, which relies on split-GFP fragment targeted to each side of the synapse [58,59]. I found that GFP signals are localized along AMB axons at the sites of MDN contact (Figs. 5, 8, and 9). These data strongly suggest that AMB axons form synaptic connections with MDN dendrites.

**AMBs are functionally presynaptic to MDNs**

Next, to investigate the functional connection between AMBs and MDNs, I performed $Ca^{2+}$ imaging of MDNs upon AMB activation. To this end, I expressed CsChrimson in AMBs and a calcium sensor GCaMP6m in MDNs and monitored $Ca^{2+}$ responses at MDN axons following optogenetic AMB stimulation (Fig. 10). In a semi-intact preparation of the larval CNS [35], red light application significantly increased GCaMP6m signal intensity in MDN axons compared with before stimulation or control animals (Fig. 10D; + CsChrimson, 4.97% ± 0.74% elevation of $\Delta F/F_0$ on average; n = 34; -CsChrimson, 0.09% ± 0.60% elevation of $\Delta F/F_0$ on average, n = 24). These data indicate that AMB activation induces $Ca^{2+}$ elevation in MDNs, supporting the idea that AMBs are functionally coupled to MDNs.

**AMBs are functionally dependent on MDNs to induce backward locomotion**

Finally, I asked whether MDNs might function downstream of AMBs to evoke backward locomotion. To test this possibility, I simultaneously activated AMBs with CsChrimson and silenced MDNs via expression of the tetanus neurotoxin light chain (TNT) (Fig. 11A) [60]. Silencing MDNs significantly decreased the number of backward waves triggered by AMB activation compared with control (Fig. 11D; Effector control, 3 in the median, n = 15; MDN-ACh-GAL4 silencing, 1 in the

median, n =17), whereas silencing MDNs did not significantly affect the number of forward waves before AMB activation (Fig. 11E; Effector control, 3 in the median; MDN-ACh-GAL4 silencing, 2 in the median). Furthermore, behavioral ethograms of AMB activation (R60F09>CsChrimson) and AMB activation with MDN silencing (R60F09>CsChrimson, MDN-ACh>TNT) showed that silencing MDN preferentially attenuated backward locomotion evoked by optogenetic AMB activation, but not other behaviors including bending and stop (Figs 11F and 11G; R60F09>CsChrimson, percentage of time spent on bending 10 seconds after light stimulation onset 24.0% in the median, stop 21.0%, n = 17; R60F09>CsChrimson, MDN-ACh>TNT; bending 37.8%, stop 28.5%, n = 14). These results indicate that AMBs trigger backward locomotion through MDNs, and silencing MDNs does not significantly affect other behavior modes induced by optogenetic activation of AMBs.

Silencing MDNs significantly reduced backward waves induced by activation of AMBs; however, it could not abolish them. There are two possibilities to explain that. One is that silencing by TNT is incomplete to inhibit signal transmission from MDNs. Another is that AMBs have an MDN-independent pathway to induce backward waves. I tested the former possibility by activating MDNs by CsChrimson and silencing MDNs by TNT at the same time (Fig. 11H). As activation of R73F04-LexA-labeled neurons induces a smaller number of backward locomotion than R60F09-LexA-labeled neurons does due to its weak labeling, I analyzed behavior in 30 seconds, which is longer than 10 seconds in R60F09-LexA activation assay in order to balance the number of backward waves induced by optogenetic activation. As a result, silencing MDNs by TNT completely abolishes backward waves induced by the activation of MDNs itself (Fig. 11I). Thus, I concluded that the latter possibility is more likely than the former one. In the latter explanation, I could not exclude the possibility that the AMB connection to the MDN-independent pathway was an artifact from silencing MDNs in the developmental stage. Taking this possibility into consideration, I conclude that AMB activation triggers backward locomotion at least in part through MDN activity. Taken together with my anatomical and functional imaging results, these data indicate that AMBs function upstream of

MDNs to evoke backward locomotion.

**Dead-end-induced backward locomotion requires neither MDNs nor AMBs**

Given that AMBs are sufficient to trigger backward locomotion, I next performed silencing experiments to test whether AMBs are required for backward locomotion in response to sensory stimuli. Previous studies showed that MDNs are required for the dead-end induced backward walking in the adult flies [24]. I, therefore, examined whether MDNs and AMBs were similarly involved in the dead-end induced backward responses in larvae using a narrow chamber ("dead-end") that limits larval lateral and rotational movements. First, I confirmed whether I could induce backward locomotion by a dead-end tube in the larval stage. When the effector control larvae encountered the end of the narrow chamber, they tried crawling forward several times and then changed their crawling direction to backward (Fig. 12). Next, I examined whether responses are mediated by C3da neurons, C4da neurons, or BO, which are reported to sense stimuli inducing directional-changing behavior. To this end, I genetically ablated sensory neurons by expressing the pro-apoptotic genes *reaper* (*rpr*) and *head involution defective* (*hid*) [61–63] in sensory neurons, C4da neurons, BO, and C3da neurons, which are reported as involving in sensing stimuli inducing backward locomotion in the larval stage [6,27,29]. I utilize ppk-GAL4 for labeling C4da neurons, GMR-GAL4 for labeling BO, and NompC-GAL4 and 19-12-GAL4 for labeling C3da neurons, respectively. As a result, I could not detect significant effects by the ablation of either BO, C4da, or C3da neurons (Fig. 12A; Effector control, 5 in the median, n = 20; ppk-GAL4 ablation, 4 in the median, n = 20; GMR-GAL4 ablation, 6.5 in the median, n = 20; ppk-GAL4 + GMR-GAL4 ablation, 4.5 in the median, n = 20; 19-12-GAL4 ablation, 7 in the median, n = 20; NompC-GAL4 ablation 4.5 in the median, n = 20). Finally, I tested the requirements of AMBs or MDNs activity in the dead-end induced backward locomotion. I silenced AMBs or MDNs by expressing TNT using AMB-GAL4 or MDN-FLP-GAL4. Compared to control larvae, I could not detect the effect on the number of backward waves by the silence of AMB or MDN (Fig. 12B; Effector control, 4 in the median, n = 20;

AMB-GAL4 control, 3 in the median, n = 20; AMB-GAL4 silencing, 3 in the median, n = 20; MDN-FLP-GAL4 control, 4.5 in the median, n = 20; MDN-FLP-GAL4 silencing, 4.5 in the median, n = 20). These results suggest that, unlike the adult, dead-end-induced backward locomotion is mediated by the AMB/MDN-independent pathway.

**Gentle touch-induced backward locomotion requires MDNs but not AMBs**

Previous studies indicate that two different stimuli can evoke backward locomotion in larvae: mechanical stimuli [6] and blue light irradiation [27] on the head. First, I asked for the requirement of neuronal activity of AMBs and MDNs in backward locomotion by mechanical stimuli. To examine the relative contribution of C3da and C4da mechanosensory neurons to the gentle touch-induced backward waves, I ablated each of them alone via expression of *rpr* and *hid*. I found that C3da ablation resulted in a significant decrease in the number of backward waves (Fig. 13A; Effector control, 1 in the median, n = 15; 19-12-GAL4 ablation, 0 in the median, n = 30; NompC-GAL4 ablation, 0 in the median, n = 30) while C4da ablation resulted in a significant increase in the number of backward waves (Fig. 13A; ppk-GAL4 ablation, 2 in the median, n = 15). This result suggests that C3da neurons, but not C4da, act to induce backward locomotion in response to gentle touch.

Next, I asked for the requirement of neuronal activity of AMBs and MDNs in gentle touch-induced backward locomotion. To this end, I selectively expressed TNT in AMBs or MDNs to silence them and monitored its effects on gentle touch-induced locomotion. Compared with effector or GAL4 controls, silencing MDNs significantly decreased the probability of animals exhibiting backward waves in response to gentle touch (Fig. 13B; Effector control, 2 in the median, n = 21; MDN-FLP-GAL4 control, 1 in the median, n = 31; MDN-FLP-GAL4 silencing, 0 in the median, n = 37). By contrast, silencing AMBs had no measurable effect on the probability of animals exhibiting backward waves (Fig. 13B; AMB-GAL4 control, 2 in the median, n = 30; AMB-GAL4 silencing, 2 in the median, n = 30). These data indicate that MDNs, but not AMBs, are required to evoke backward locomotion upon gentle touch.

**Blue light-induced backward locomotion requires MDNs, but not AMBs**

Finally, I asked for the requirement of neuronal activity of AMBs and MDNs in backward locomotion induced by blue light irradiation[27]. Previous studies suggested that two distinct sensory systems, the BO and the C4da neurons, mediate this behavioral response to blue light [29,42]; however, how these two distinct pathways are integrated to drive backward locomotion remains unknown. To examine the relative contribution of BO, C4da, and C3da neurons to the blue light-induced backward waves, I genetically ablated each of them alone or in combination via expression of *rpr* and *hid*. I found that ablation of both BO and C4da neurons caused a significant reduction in the probability of animals exhibiting backward waves compared to the effector control, while the probability of animals exhibiting backward waves was unaffected by ablation of either BO or C4da neurons alone (Fig. 14A; Effector control, 56.7%, n = 30; ppk-GAL4 ablation, 53.3%, n = 30; GMR-GAL4 ablation, 33.3%, n = 30; ppk-GAL4 + GMR-GAL4 ablation, 7.4%, n = 27). I also assessed whether C3da neurons could contribute to blue light-induced backward locomotion, as some studies also reported that C3da neurons work together with C4da neurons to induce backward locomotion [27]. I found that ablating C3da neurons or combination of C3da neurons and BO did not result in significant change in the probability of animal existing backward waves compared to the effector control (Fig. 14A; 19-12-GAL4 ablation, 30%, n = 30; NompC-GAL4 ablation, 45.2%, n = 31; 19-12-GAL4 + GMR-GAL4 ablation, 26.7%, n = 30; NompC-GAL4 + GMR-GAL4 ablation, 53.3%, n = 30). Thus, BO and C4da pathways, but not C3da, function redundantly to trigger blue light-induced backward locomotion.

I next asked for the requirement of neuronal activity of AMBs and MDNs in blue light-induced backward locomotion. To this end, I selectively expressed TNT in AMBs or MDNs and monitored the effects of TNT expression on blue light-induced locomotion. Compared with effector or GAL4 controls, silencing MDNs significantly decreased the probability of animals exhibiting backward waves in response to blue light stimulation (Fig. 14B; Effector control, 45.7%, n = 35; MDN-FLP-

GAL4 control, 38.1%, n = 21; MDN-FLP-GAL4 silencing, 6.67%, n = 30). By contrast, silencing AMBs had no measurable effect on the probability of animals exhibiting backward waves (Fig. 14B; AMB-GAL4 control, 33.3%, n = 30; AMB-GAL4 silencing, 43.3%, n = 30). These data indicate that MDNs, but not AMBs, are required to evoke backward locomotion upon blue light irradiation.

Blue light irradiation causes not only backward locomotion but also another repertoire of escape behavior such as bending [29]. Thus, I tracked larval behavior during blue light irradiation for each genotype. As a result, I found that the behavioral sequence was mostly unaffected by AMB or MDN silencing (Fig. 15). These data together suggest that the AMB-MDN pathway specifically involves in the regulation for backward locomotion.

**C4da-induced backward locomotion requires AMB-MDN pathway**

Given that BO and C4da pathways function redundantly to evoke backward locomotion upon blue light irradiation and AMBs are presynaptic to MDNs, I reasoned that AMBs might specifically relay information from either the BO or the C4da pathway to MDNs. To test this hypothesis, I first test whether AMBs or MDNs have a direct connection with sensory neurons. I dual-labeled BO or C4da neurons with MDNs or AMBs. I observed no direct connections between the sensory neurons and the AMB-MDN pathway (Fig. 16). Thus, I decided to focus on the functional connection between the AMB-MDN pathway and the sensory pathways. To examine the functional connection between them, I conducted behavior assay and functional imaging assay.

First, I test whether optogenetic activation of either BO or C4da neurons could induce backward locomotion using Rh6-LexA and R27H06-LexA to drive specific expression of CsChrimson in BO and C4da neurons, respectively [35,64]. I found that optogenetic activation of C4da neurons induced multiple escape behaviors, including bending, rolling, and backward locomotion (bending 100% of observed larvae, rolling 55.0 %, backward locomotion 35.0 %, n = 40). During optogenetic C4da activation for 30 seconds, rolling tended to be evoked in the earlier time (0-5 seconds), whereas backward locomotion was observed in the later time (5-30 seconds). Similarly, optogenetic activation

of BO evoked bending and backward locomotion, but not rolling (bending 100% of observed larvae, backward locomotion 32.5%, n = 40).

Next, I assayed the effects of MDN or AMB silencing on optogenetically induced backward locomotion by TNT expression. In this experiment, I utilized two AMB-labeling GAL4 lines (R60F09-ACh-GAL4, R73D06-GAL4) because of the difficulty in putting all transgenes together in AMB-GAL4 (splitGAL4) background. Silencing MDNs significantly decreased the probability of animals exhibiting backward locomotion induced by BO or C4da neuron activation (Fig. 17; C4da activation with MDN-FLP-GAL4 silencing, 5.0%, n = 40; BO activation with MDN-FLP-GAL4 silencing, 7.5%, n = 40), consistent with a previous report that MDNs are command-like neurons for noxious touch-induced backward waves [6]. Silencing AMBs similarly decreased the probability of animals exhibiting backward waves in response to activation of C4da neurons (Fig. 17; C4da activation with R60F09-ACh-GAL4 silencing, 7.5%, n = 40; C4da activation with R73D06-GAL4 silencing, 7.1%, n = 42). However, backward waves induced by BO activation were largely unaffected by silencing AMBs (Fig. 17; BO activation with R60F09-ACh-GAL4 silencing, 35.0%, n = 40; BO activation with R73D06-GAL4 silencing, 36.7%, n = 30). These data together suggest that AMBs mediate C4da-induced backward locomotion, but not BO-induced one.

**C4da neurons evoke $Ca^{2+}$ responses in AMBs**

Finally, in order to confirm the functional connection between AMBs and sensory organs, I asked whether activation of either BO or C4da neurons could trigger $Ca^{2+}$ responses in AMBs. I expressed GCaMP6m in AMBs and CsChrimson in sensory neurons and monitored $Ca^{2+}$ responses in AMBs following BO or C4da activation. Optogenetic activation of C4da neurons, but not BO, resulted in a significant increase of GCaMP6m fluorescence intensity in AMB somas (Figs. 18A-18D; +CsChrimson, 6.89% ± 1.46% elevation of $\Delta F/F_0$ on average; n = 37; -CsChrimson, 0.21% ± 1.09% elevation of $\Delta F/F_0$ on average, n = 16. Figs. 18E-18H; +CsChrimson, 0.98% ± 1.71% elevation of $\Delta F/F_0$ on average; n = 23; - CsChrimson, 0.33% ± 0.86% elevation of $\Delta F/F_0$ on average, n = 22),

consistent with the idea that AMBs mediate noxious information from C4da neurons, but not from BO.

**Physiological blue light irradiation evokes $Ca^{2+}$ responses in AMBs via C4da neurons.**

I further tested that AMBs indeed relay physiological blue light information from the C4da pathway. To this end, I expressed GCaMP6s in AMBs and irradiated blue lights to activate the C4da pathway physiologically. I found that control larvae showed a significant increase in the fluorescence intensity in AMB somas in response to blue light irradiation, whereas no significant increase of the fluorescence intensity was observed in larvae ablated C4da neurons (Fig. 19; +rpr, 0.74% ± 2.23% elevation of $\Delta F/F_0$ on average, n = 43; -rpr, 7.40% ± 3.17% elevation of $\Delta F/F_0$ on average, n = 40). This data indicates that blue light irradiation activates AMB neurons via C4da neurons. Taken together, our data indicate that AMBs preferentially convey blue light information from C4da sensory neurons to MDNs to evoke backward locomotion.

In conclusion, my data indicate that AMBs specifically convey noxious blue light information from C4da sensory neurons to MDNs in order to evoke backward locomotion (Fig. 20).

# Discussion

### The AMB-MDN pathway is involved in the C4da-induced backward locomotion

Command-like neurons for backward locomotion have been described in several animal species including AVA neurons in *C. elegans* and MDNs in *Drosophila melanogaster* [5,6,24], although it remains largely unknown how they are activated by sensory inputs. In this study, I have identified a novel class of ascending interneurons named AMBs, which activate MDNs to elicit backward locomotion in *Drosophila* larvae. This notion is supported by the following lines of evidence. First, optogenetic activation of AMBs can induce backward locomotion similar to that induced by MDN activation (Figs. 3, 4, and 7). Second, anatomical and functional analysis showed that AMBs are excitatory ascending neurons that are directly presynaptic to MDNs (Figs. 5, 6, and 8-10). Third, AMB-induced backward locomotion is largely dependent on MDN activity (Fig. 11). Previous TEM connectome studies suggested that MDNs are unlikely to receive direct inputs from sensory neurons [6]. Consistent with this idea, my data suggest that AMBs are the major presynaptic neurons that convey C4da sensory neuron-derived noxious blue light stimuli to MDNs as silencing either AMBs or MDNs attenuated C4da-induced backward locomotion to a similar degree, and AMBs receive blue light stimuli via C4da neurons (Figs. 17-19). Likewise, MDNs are likely to be the major postsynaptic neurons for AMBs to elicit backward locomotion, but I could not rule out the possibility that AMBs might have other downstream neurons to induce backward locomotion, as AMB-induced backward locomotion remained even in the larvae with silencing MDNs (Fig. 11).

### MDNs function as the convergence points

MDNs are required for backward locomotion in response to mild noxious touch to the head [6], but until now, it has not been examined whether MDNs are also required for backward locomotion in response to other sensory modalities. Here I have shown that MDNs are indeed required for backward

locomotion in response to noxious blue light irradiation as well as gentle touch (Figs. 13-14). In larvae, gentle touch and lights are typically received by different sensory systems; gentle touch is likely sensed by C3da sensory neurons, whereas noxious blue light stimulus is detected by BO and C4da sensory neurons [29,30]. I propose that MDNs are convergence points for the sensory inputs to trigger backward locomotion because AMBs are neurons that are directly presynaptic to MDNs and do not receive BO signals. The previous research and my experiment consistently support the idea that BO and C4da pathways have additive effects in the induction of escape behavior [29] (Fig. 14). The additive effects can be explained by the integration of two sensory systems in the command-like neurons, MDNs. Thus, my present results suggest that the cellular mechanism of MDNs for integrating distinct sensory inputs is a good target to investigate the mechanism to enable appropriate decision making in escape behavior repertoires. It is also interesting to examine whether other noxious sensory modalities, such as high temperature, high salt, and bitter taste, might also require MDNs to evoke escape behavior including backward locomotion.

Furthermore, it is of importance to examine whether AMBs specifically mediate noxious light information or are also recruited by inputs from the other sensory modalities. The possibility cannot be excluded that AMBs receive inputs from C3da neurons even though it is unlikely that the AMB-MDN pathway functions as the main downstream of C3da neurons (Fig. 13). If that is the case, AMBs also might function as the convergence point of different sensory pathways and control the escape behavior in response to a specific environmental cue as shown in multimodal integration of rolling circuits [37,38].

**The pathways involved in backward locomotion potentially function in parallel**

A previous report suggests that the anterior Wave neurons likely send outputs to motor circuits in the VNC to promote backward locomotion and do not require the brain to induce backward waves [27]. Although the functional relationship between Wave neurons and MDNs has not yet been examined, it is likely that these two pathways can work in parallel. It is possible that specific

behavior is controlled by two independent circuits. For example, the other type of escape behaviors rolling controlled by neural circuits downstream of C4da neurons, have the brain-pathway and the VNC-pathway [35,36]. Thus, it may be true for backward locomotion pathways to have AMBs and MDNs in the brain pathway and Wave neurons in the VNC pathway. The backward locomotion circuits in the brain consist of small subsets of neurons, implied by the results that my optogenetic screening identified only 11 GAL4 lines out of 783 GAL4 lines, which induced robust backward locomotion. My screening possibly failed to identify backward-inducing neurons in the VNC, whose labeling was inhibited by tsh-GAL80. As expected, I could not identify GAL4 lines labeling anterior Wave neurons whose activation induce backward locomotion because the GAL4 labeling of Wave neurons was diminished by tsh-GAL80 [27]. Thus, there could be more neurons inducing backward locomotion in the VNC; however, my data reveals that backward locomotion circuits in the brain consist of small subsets of neurons.

Additionally, it is also shown that there is an MDN-independent pathway to induce backward locomotion in response to a dead-end. The behavioral assay indicated that none of the sensory neurons tried (C4da, C3da, and BO), and the AMB-MDN pathway had a significant effect on dead-end-induced backward locomotion (Fig. 12). Thus, this dead-end-induced pathway is also independent of the Wave pathway. This result suggests that AMBs and MDNs do not work in general backward circuits like motor circuits, but function only in specific backward circuits. It was a surprising result for me because adult MDN neurons have been reported to be required for dead-end-induced backward locomotion and sense a dead-end via TLA neurons using NompC positive mechanosensory neurons [24,25]. It could come from the difference between ways to sense a "dead-end" in the larval stage and the adult stage. This study used narrow chambers to avoid larval escape just by turning and forward run behavior because larvae prefer to choose turning and forward run than backward locomotion when there is room to bend their head, according to my observation. On the other hand, adult studies used the relatively wider chamber to make room for the movement of legs compared with the one used in this study. This could make a difference in a way to sense a dead-end in each

study. In my experiment, larvae can sense a dead-end in two ways. One is mechanosensory inputs toward the body wall from the tube, and the other is the situation in which "they cannot go further in spite of trials to run forward". The former sensation could be conveyed by C3da neurons. Taking into consideration the larval physiological environment where they burrow holes in their food, it is unlikely to induce backward locomotion just by mechanosensory inputs toward the entire body wall. This could explain the former signal, maybe from C3da, is not important for inducing backward locomotion in response to a dead-end in my experiment. The latter signal is possibly sensed by proprioceptors, two classes of arborizing multidendritic sensory neurons known as the class I neurons (md-I) and the bipolar md neuron [23,38,65,66]. These sensory neurons are active during forward or backward muscle contraction waves [66]. The larval movement needs their feedback to detect in order to convey waves smoothly [23]. Thus, it is possible that there is an MDN-independent pathway to sense the situation that "cannot go further" by detecting abnormal feedback from proprioceptors. Consistent with this idea, a recent study reported larvae with *pzl* mutant or loss of function of Cho neurons, whose proprioceptor could have an abnormal function, showed more turning and repetitive backward waves [77]. Further study will be needed to elucidate which sensory neurons convey signals in this assay and to elucidate how the potentially parallel pathways are coordinated to execute the appropriate behavioral response.

**The AMB-MDN pathway is involved in the backward locomotion, but not in the other escape behavior**

Blue light can induce multiple different repertoires of escape behavior, including forward run, bending, and backward locomotion, presumably through multiple downstream circuits [67,68]. In addition, my data indicate that the AMB-MDN pathway for backward locomotion is independent of the pathways required for the other types of escape behaviors, as behavioral sequences of forward run and bending were largely unaffected by silencing AMBs and MDNs (Figs. 11 and 15). It, therefore, remains to be elucidated how different modality of noxious sensation evokes distinct repertories of

escape behavior through activating C4da neurons and the downstream pathways. One potential mechanism is antagonistic systems between the downstream circuits [9,67,69,70]. An alternative scenario is that C4da neurons could provide distinct signals to the secondary neurons in response to different modalities. Previous studies suggested that noxious heat and blue lights can evoke different firing patterns in C4da neurons [68]. It is thus possible that C4da neurons might preferentially recruit particular secondary neurons through specific firing patterns, thereby evoking specific escape behavior.

**Interspecific comparison of backward circuits**

The convergence of distinct sensory modalities has also been reported in the other command neurons. AVA neurons, the backward command neurons in *C. elegans*, receive inputs from multiple modalities such as anterior mechanosensory inputs from AVM/ALM disynaptically or nociceptive inputs from ASH monosynaptically [18,71–75]. Thus, the convergence of several different sensory modalities is considered as a shared feature of the command-like neuron controlling locomotion directions. MDNs do not directly receive sensory inputs in contrast to AVA neurons. It might enable MDNs to cope with a complex situation to induce backward locomotion. AVA neurons receive direct inhibitory inputs from PLM, which detect posterior body touch [75]. A previous study indicated that MDNs inhibit forward locomotion via downstream circuits [6], although it is not analyzed whether MDNs get inputs from forward locomotion circuits. It may be interesting to examine whether MDNs receive inhibitory inputs from neurons inducing forward locomotion and compare the circuits mechanisms among different species.

**Comparison between the adult and the larval MDN circuit**

The previous study reported that MDNs function as command-like neurons from the larval stage to the adult stage, although it remains to be elucidated whether the circuit mechanism of MDNs also

persists in the adult stage [6]. Recent studies have revealed upstream of the adult MDNs, LC16 neurons mediating visual inputs, and TLA neurons in mechanosensory inputs [25,26]. Here, I identified AMBs as upstream neurons mediating C4da inputs to the larval MDNs. Interestingly, all the neurons upstream of MDNs identified so far receive modality-specific signals. This implies shared features between MDNs in the adult stage and those in the larval stages. Furthermore, it is reported that some of the sensory neurons persist in the adult stage, while others are eliminated during metamorphosis [76]. It should be noted that C4da neurons have been reported to be one of the neurons that persist in the adult stage. Thus, it should be tempting to see whether the AMB-MDN pathway also persists into adulthood and function to induce backward locomotion. I believe that my present thesis will pave the way for the direct comparison of the neural circuit mechanisms for the behavior having the same role in the adult and the larval stage.

**Conclusions**

In conclusion, by the use of functional optogenetic and in vivo imaging techniques in the larval nociceptive circuits, I have revealed a circuit mechanism by which distinct sensory pathways are integrated to evoke backward locomotion. It can explain the additive effect of redundant visual pathways, which induce escape behavior by integrating two pathways in MDNs. I propose that the results of my present thesis should contribute to the elucidation of the neural circuit-based mechanism of how multiple sensory inputs are integrated to regulate specific behavior.

# Figures

**Table. 1. Genotypes of GAL4 lines utilized in this study.**

| GAL4 abbreviation | Genotype |
|---|---|
| R60F09-ACh-GAL4 | VGlut-GAL80 [MI04979]; R60F09-GAL4 |
| R60F09-Brain-GAL4 | Otd-FLPo, tub-FRT-GAL80-FRT; R60F09-GAL4, tub-GAL80$^{ts}$ |
| AMB-GAL4 | R60F09-GAL4DBD, R11E07-p65AD |
| MDN-ACh-GAL4 | tsh-GAL80; R73F04-GAL4, Gad1-2A-GAL80 |
| MDN-FLP-GAL4 | Otd-FLPo, tub-FRT-GAL80-FRT; R73F04-GAL4, Gad1-2A-GAL80 |

**Fig. 1. Organization of the larval sensory systems.**

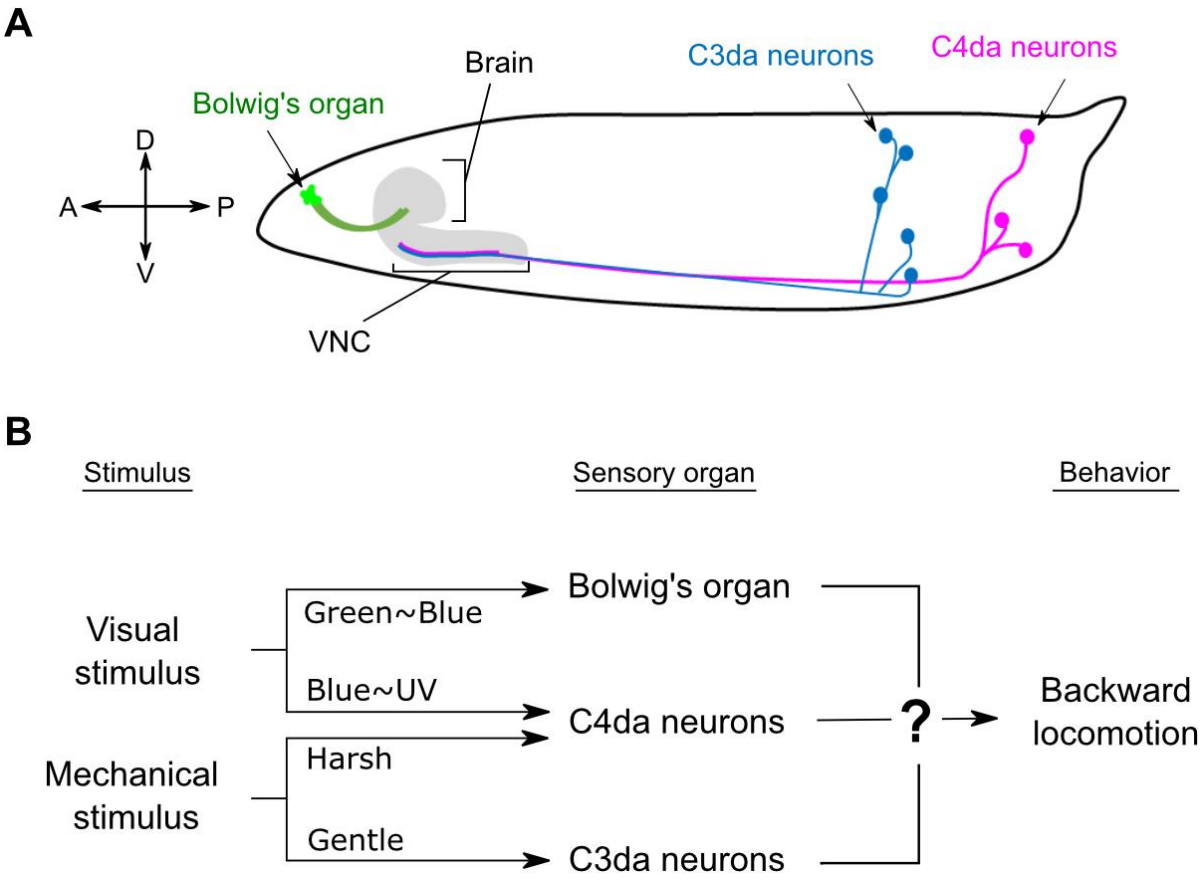


(A) Localization and project sites of the larval sensory neurons. BO shown in green is located in the head and projects to the brain. C3da neurons shown in blue and C4da neurons shown in

magenta. C3da and C4da neurons cover the entire body wall and project to the VNC. (B) Sensory pathways to induce backward locomotion. In the visual pathway, BO receives green to blue light irradiation while C4da neurons receive blue to UV irradiation at high intensity. In the mechanical pathway, C4da neurons receive harsh touch while C3da neurons receive gentle touch. It remains largely unknown how these sensory pathways are integrated to induce backward locomotion.

**Fig. 2. R73F04-GAL4 and R73F04-LexA label MDNs.**

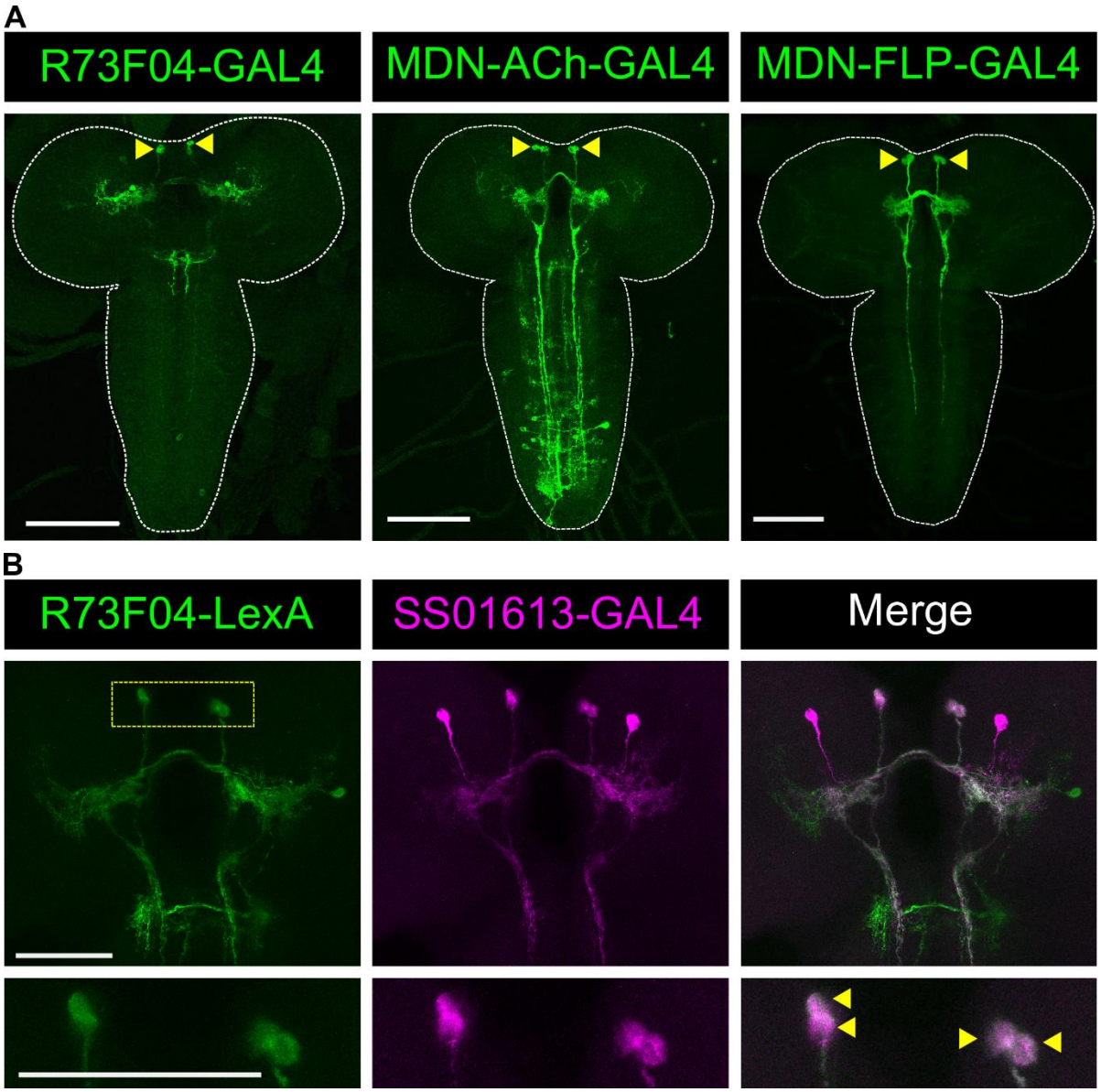


(A) Expression patterns of MDN-labeling GAL4 used in this study. The yellow arrowheads indicate the soma of MDNs. Genotypes: w; UAS-mCD8GFP, tsh-GAL80/+; R73F04- GAL4/+ (R73F04-GAL4); w; UAS-mCD8GFP, tsh-GAL80/+; R73F04-GAL4, Gad1-2A- GAL80/+ (MDN-ACh); w; UAS-mCD8GFP/Otd-FLPo, tub-FRT-GAL80-FRT; R73F04- GAL4, Gad1-

2A-GAL80/+ (MDN-FLP). Scale bar, 100 μm. (B) Dual-labeling with MDN- labeling GAL4 used in the previous study (SS01613-GAL4) [6] and R73F04-LexA. The yellow dotted square in the upper row indicates the area shown in the lower row. The yellow arrowheads indicate both R73F04-LexA and SS01613-GAL4 label the soma of MDNs. Scale bar, 50 μm.

**Fig. 3. AMBs are a pair of neurons in SEZ that can induce backward waves upon optogenetic activation.**

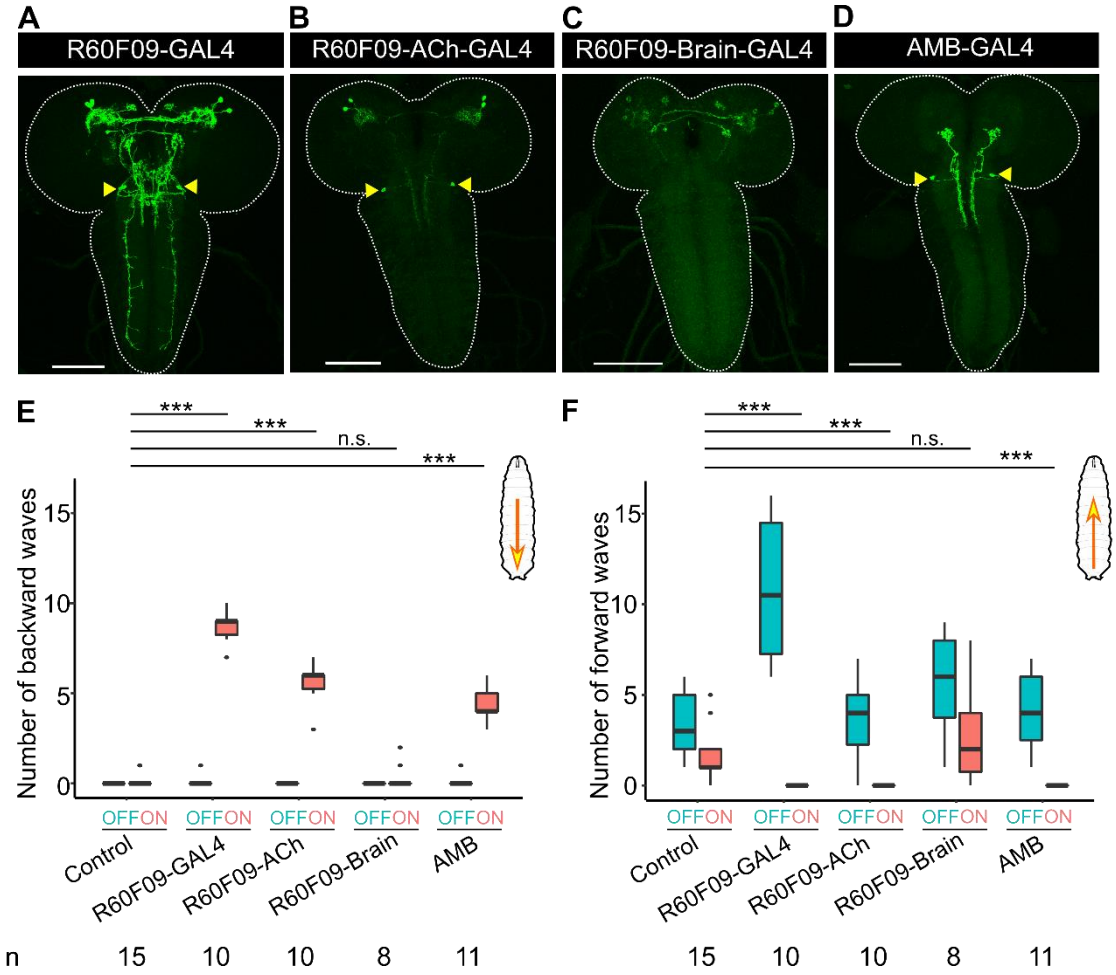


(A-D) Expression patterns of GAL4 lines. The yellow arrowheads indicate the somas of AMBs. Scale bar, 100 μm. Genotypes of each GAL line are shown in Table. 1. (E, F) The number of backward/forward waves in 10 seconds before (OFF) or during (ON) optogenetic activation with CsChrimson. Genotypes: w; UAS-CsChrimson/+; +/+ (Control); other four lines drive CsChrimson by GAL4 lines shown in (A-D) In the boxplot, the width of the box represents the interquartile range. The whiskers extend to the data point that is less than 1.5 times of the length of the box away from the box, and the dot represents the outlier. I assessed statistical significance using the Wilcoxon rank-sum test

and corrected for multiple comparisons using the Holm method. ***p<0.001.

**Fig. 4. R60F09-LexA and R73D06-GAL4 label AMBs.**

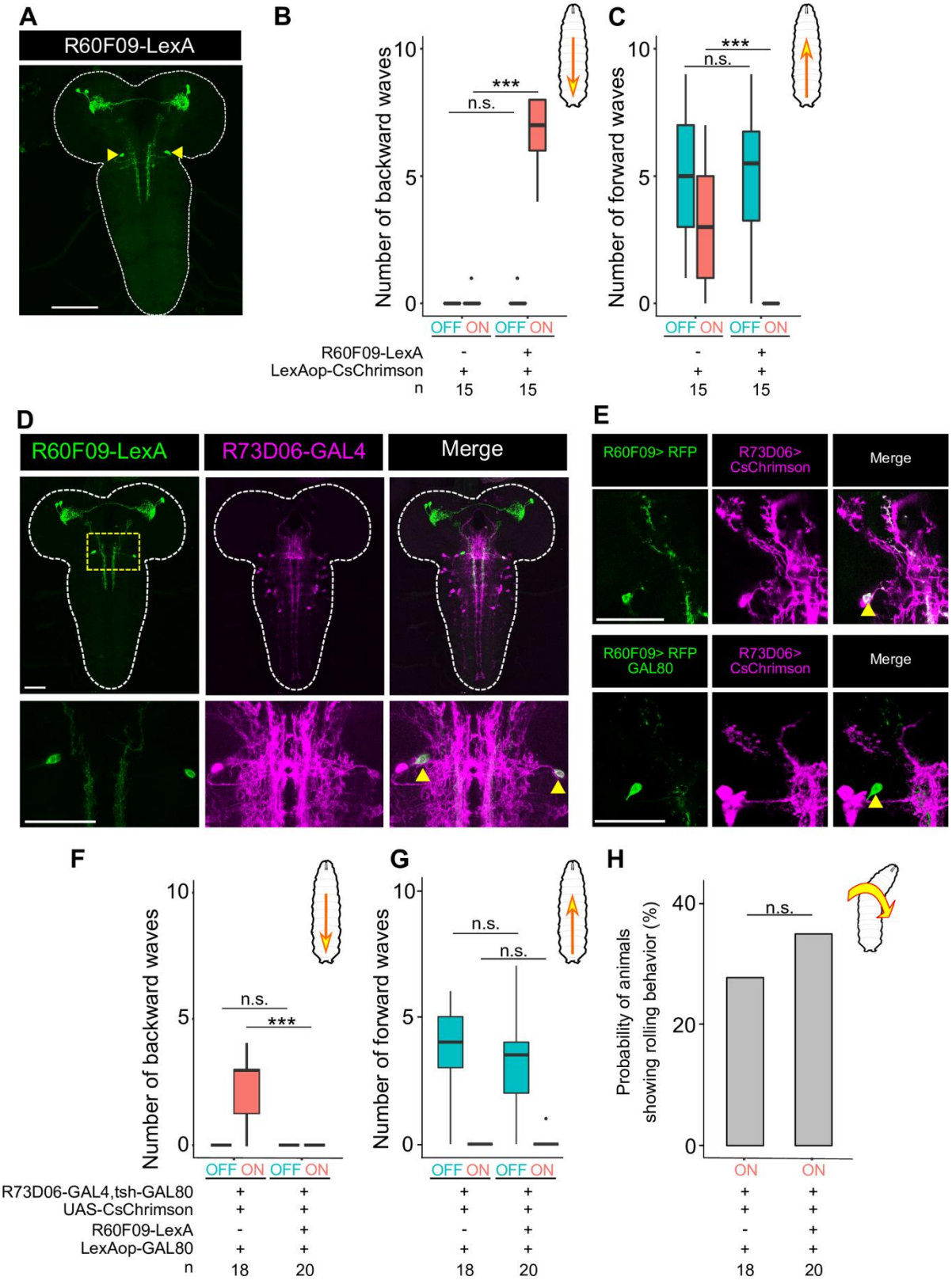

(A) Expression patterns of R60F09-LexA in the third instar larval CNS. The yellow arrowheads indicate the soma of AMBs. Maximum intensity projection of the entire CNS shown. Genotypes: LexAop-mCD8GFP, UAS-mCD8RFP/+; R60F09-LexA/+; +/+. Scale bar, 100 μm. (B, C) The number of backward/forward waves in 10 seconds before (OFF) or during (ON) optogenetic activation with CsChrimson. I assessed the statistical significance by the Wilcoxon rank-sum test with the Holm method. ***p < 0.001. (D) R60F09-LexA and R73D06-GAL4 co-label AMBs. The yellow dot square indicates the area shown in the lower row. The yellow arrowheads indicate the somas of AMBs. Genotypes: LexAop-mCD8GFP, UAS-mCD8RFP/+; R60F09-LexA/+; R73D06-GAL4/+. Scale bars, 50 μm. (E) GAL80 labeled by R60F09-LexA diminishes CsChrimson expression in AMBs labeled by R73D06-GAL4 co-labeling. The yellow arrowheads indicate the somas of AMBs. Genotypes: w; LexAop-rCD2RFP/R60F09-LexA, tsh-GAL80; R73D06-GAL4/UAS-CsChrimson (the upper row), w; LexAop-rCD2RFP/R60F09-LexA, tsh-GAL80; R73D06-GAL4/UAS-CsChrimson, LexAop-GAL80 (the lower row). Scale bars, 50 μm. (F, G) The number of backward/forward waves in 10 seconds before (OFF) or during (ON) optogenetic activation with CsChrimson. In the boxplot, the width of the box represents the interquartile range. The whiskers extend to the data point that is less than 1.5 times the length of the box away from the box, and the dot represents an outlier. I assessed the statistical significance by the Wilcoxon rank-sum test with the Holm method. ***p < 0.001. (H) Probability of animals showing rolling behavior in 10 seconds before (OFF) or during (ON) optogenetic activation with CsChrimson. I assessed the statistical significance by Fisher's exact test.

**Fig. 5. Anatomical characterization of AMBs and MDNs.**

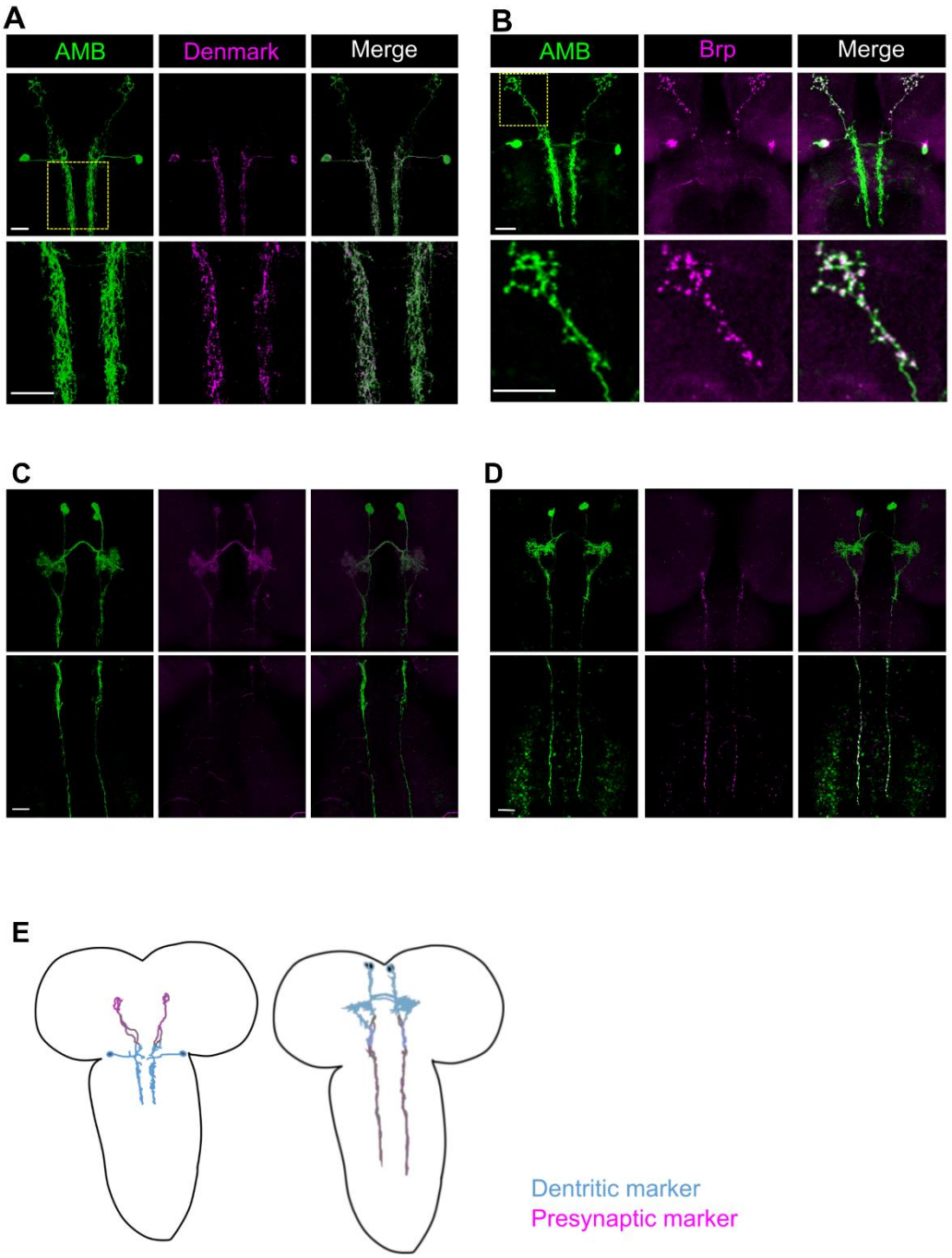


(A, B) Anatomical characterizations of AMBs. The yellow dotted square indicates the area shown in the lower row. The dendritic marker Denmark (A) shows AMBs have dendrites in the VNC, and the presynaptic marker BrpD3::mCherry (B) shows AMBs have ascending

axons to the brain. Genotypes: w; UAS-mCD8GFP/VGlut-GAL80 [MI04979]; R60F09-GAL4/UAS-Denmark (A); w; UAS-mCD8GFP/VGlut-GAL80 [MI04979]; R60F09-GAL4/UAS-BrpD3::mCherry (B). (C, D) Anatomical characterizations of MDNs. The upper row shows MDN neurites in the brain, and the lower row shows those in the VNC. The dendritic marker Denmark (C) shows MDNs have dendrites in the brain, and the presynaptic marker BrpD3::mCherry (D) shows MDNs have descending axons to the VNC. Genotypes: w; UAS-mCD8GFP/Otd-FLPo, tub-FRT-GAL80-FRT; R73F04-GAL4, Gad1-2A-GAL80/UAS-Denmark (C); w; UAS-mCD8GFP/Otd-FLPo, tub-FRT-GAL80-FRT; R73F04-GAL4, Gad1-2A-GAL80/UAS-BrpD3::mCherry (D). Scale bar, 20 μm. (E) The schematic anatomy of AMBs and MDNs. The color of neurites indicates the soma and the dendritic arbors (blue) and presynaptic site in the axonal processes (magenta), presumed by genetic markers.

**Fig. 6. AMBs are immunoreactive to ChAT, but not to VGluT and GABA.**

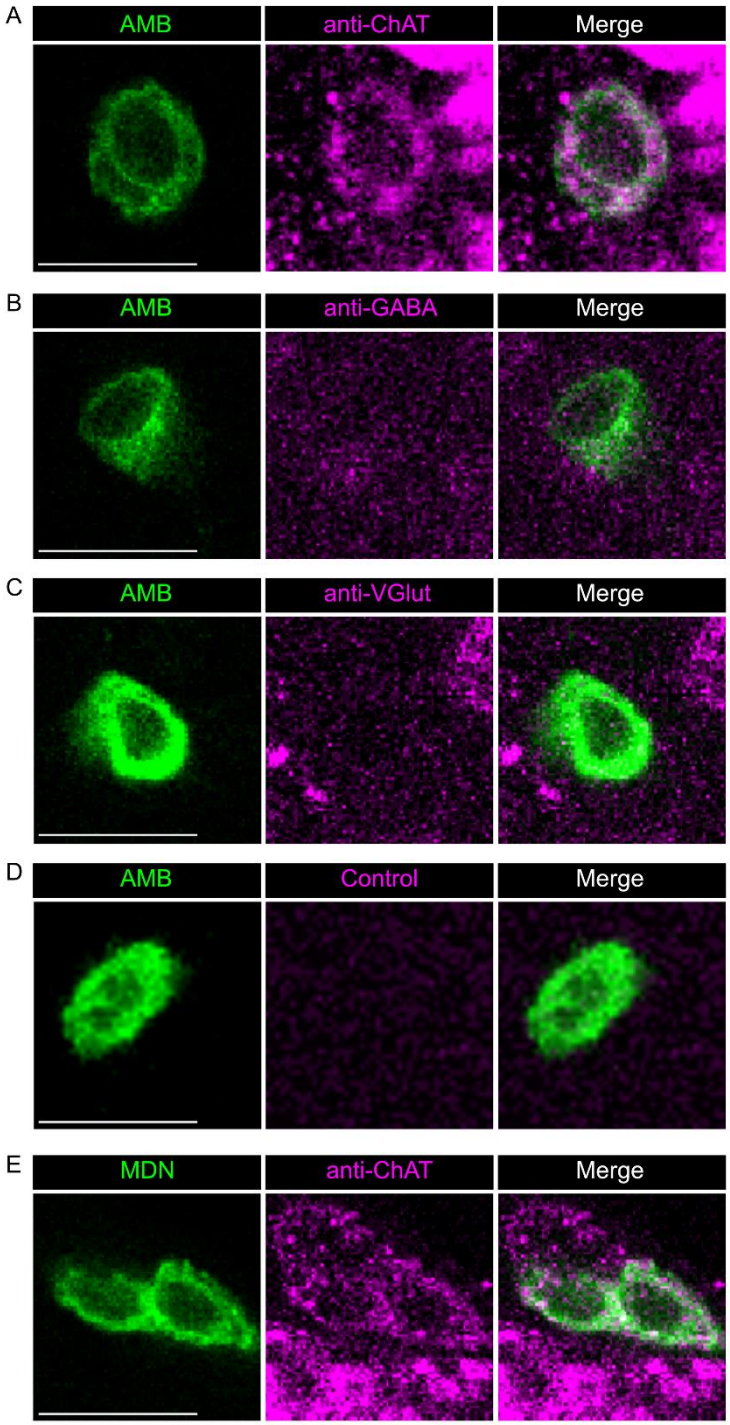

(A-C) AMBs are labeled with membrane-localized GFP and immunostaining for neurotransmitter markers: ChAT, VGluT, and GABA. (D) Negative control of 2nd antibodies for immunohistochemistry. No detectable immunostaining was observed in AMB somas without anti-ChAT antibody. (E) Positive control for anti-ChAT. Anti-ChAT stained MDN somas that were reported to be cholinergic neurons in the previous study [6]. Scale bars, 10 μm.

**Fig. 7. Optogenetic activation of AMBs or MDNs triggers similar repetitive backward waves.**

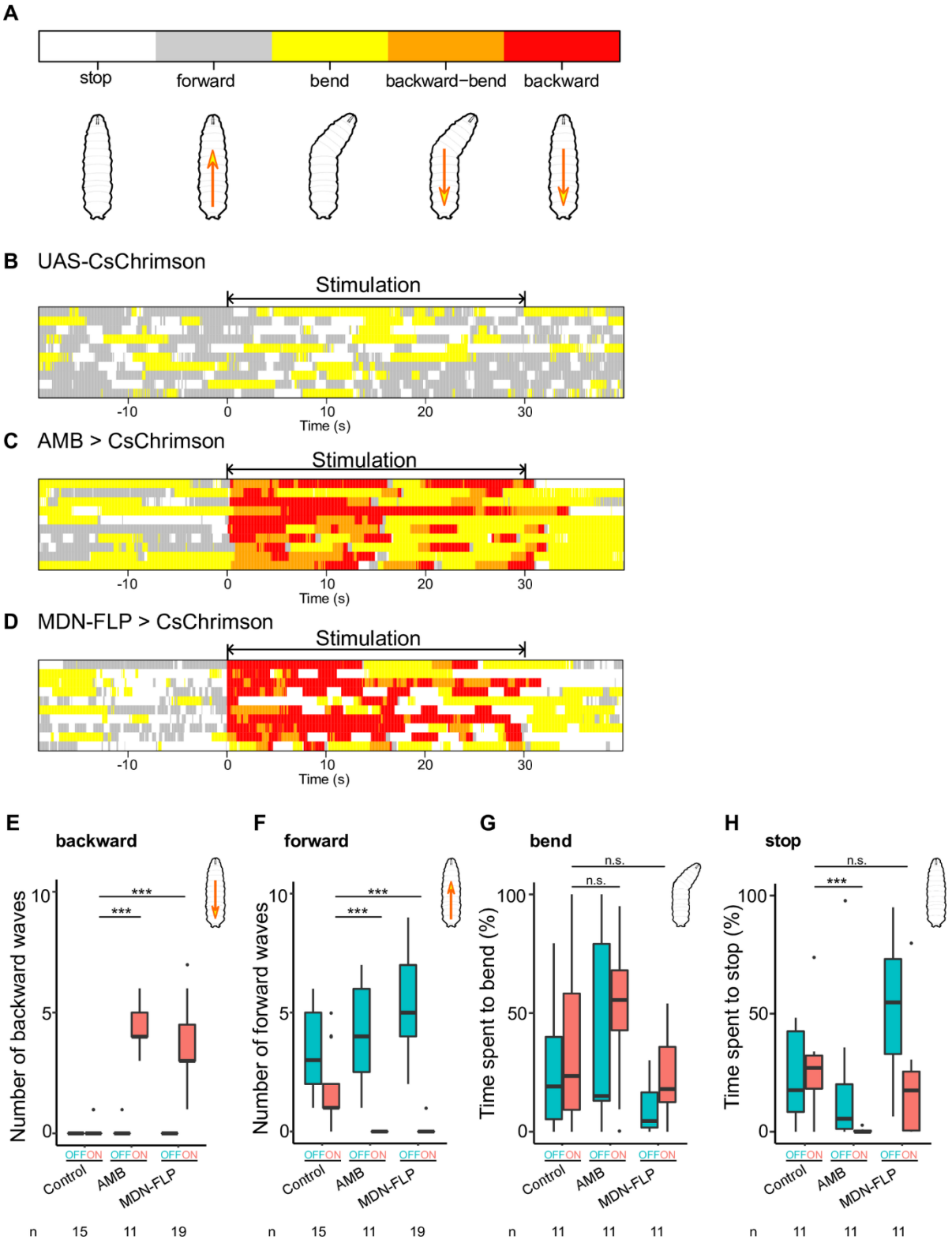

(A) Behavior events are color-coded: forward movement (grey), stop (white), bending (yellow), bending with backward locomotion (orange), and backward locomotion (red). (B-D) Behavior ethograms upon optogenetic stimulation of AMBs or MDNs. An animal expressing CsChrimson in either population was subjected to optogenetic activation for 30 seconds. Representative data from 10 different animals are shown for each genotype. (E-H) The number of backward/forward waves or percentage of time spent in a behavioral mode in 10 seconds before (OFF) and during (ON) optogenetic AMB activation with CsChrimson while silencing MDNs. In the boxplot, the width of the box represents the interquartile range. The whiskers extend to the data point that is less than 1.5 times the length of the box away from the box, and the dot represents the outlier. I assessed the statistical significance by the Wilcoxon rank-sum test with the Holm method. ***$p < 0.001$.

**Fig. 8. AMB axons are apposed to MDN dendrites in the larval brain.**

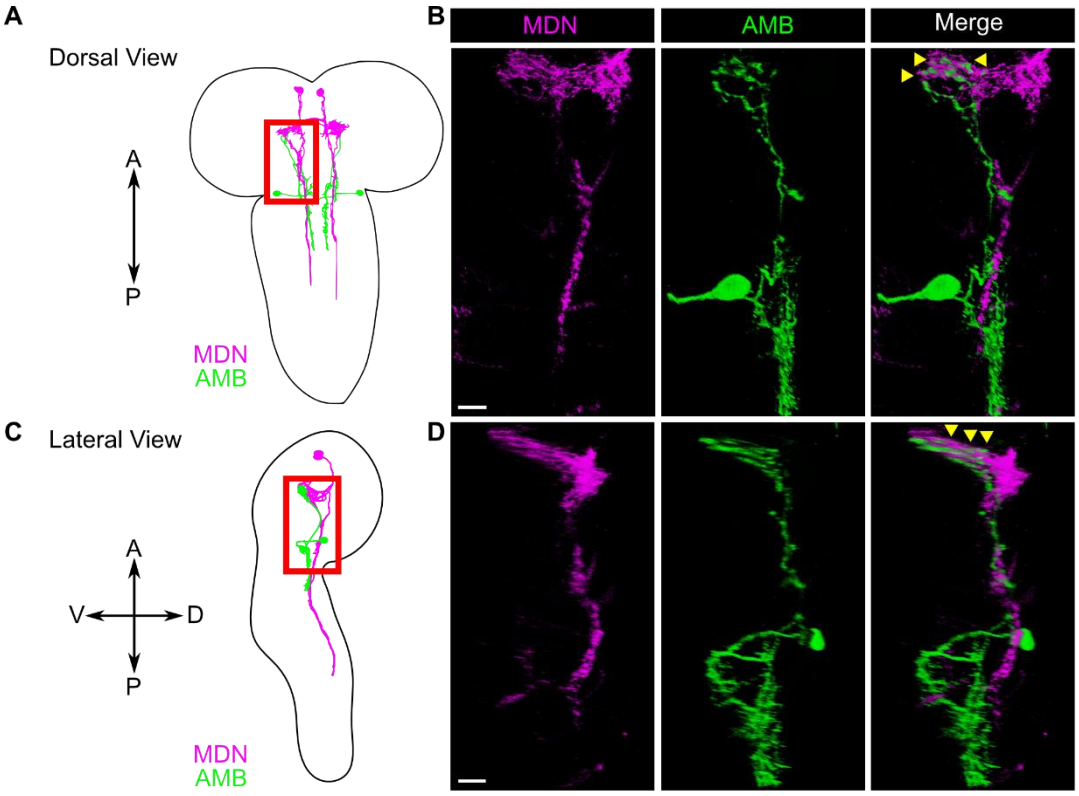


(A-D) A schematic view of AMBs and MDNs from the dorsal (A) and from the lateral side (C). The area with red boxes in (A) and (C) were shown in (B) and (D), respectively. Dual-labeling of AMBs (green) and MDNs (magenta). AMBs and MDNs were co-labeled with membrane-localized RFP and membrane-localized GFP, respectively. Genotypes: w; R60F09-LexA, tsh-GAL80/LexAop-rCD2RFP; R73F04-GAL4, Gad1-2A-GAL80/UAS-mCD8GFP. Scale bars, 10 μm.

**Fig. 9. GRASP signals are detected between AMB axons and MDN dendrites.**

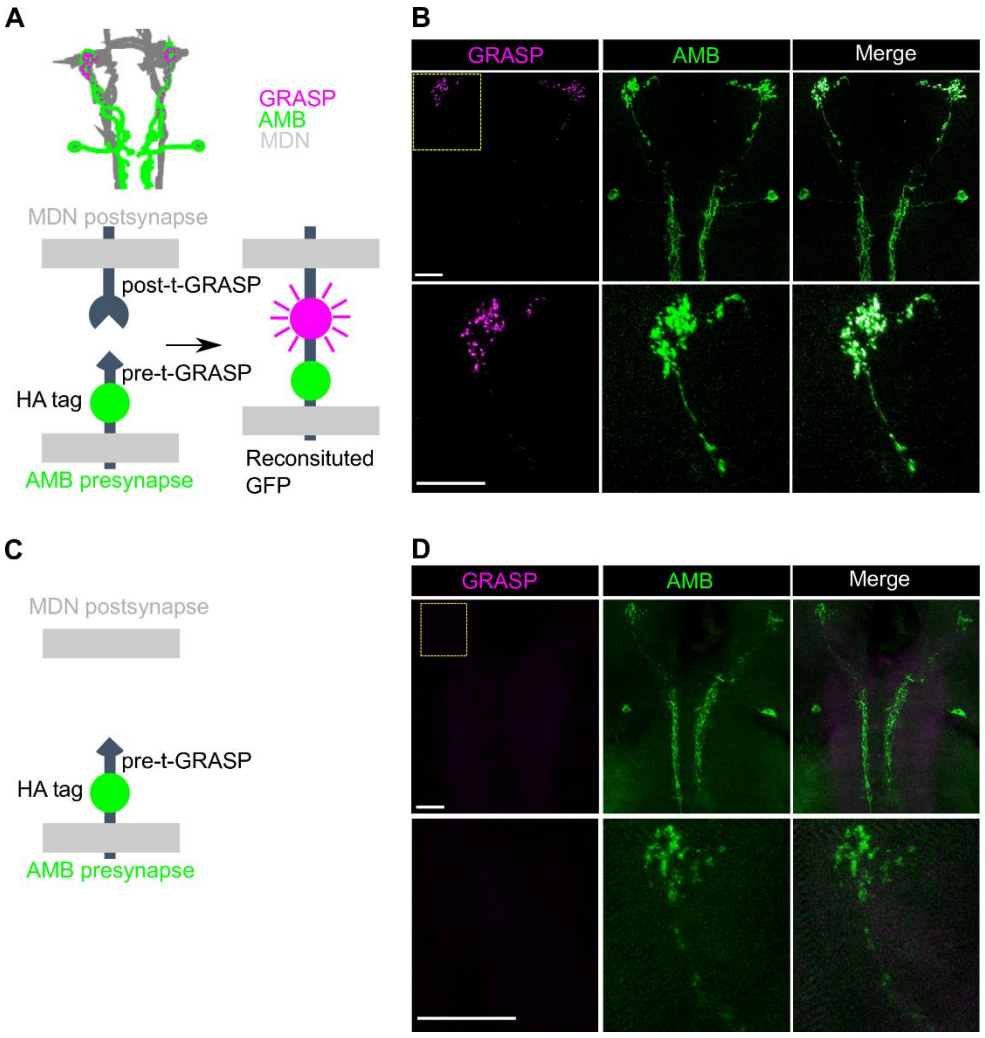


(A-B) t-GRASP between AMBs and MDNs showed signals specific to AMB axons in the brain. The yellow dotted square in the upper row indicates the area shown in the lower row. GRASP signals are shown in magenta, and AMB neurons labeled with anti-HA are shown in green. Genotypes: w; R60F09-LexA/+; R73F04-GAL4, Gad1-2A-GAL80/UAS-post-tGRASP, LexAop-pre-t-GRASP. (C-D) pre-t-GRASP in AMBs alone did not show GFP signals. Genotypes: w; R60F09-LexA/+; LexAop-pre-t-GRASP, UAS-post-t-GRASP/+. Scale bars, 20μm.

**Fig. 10. AMBs function upstream of MDNs.**

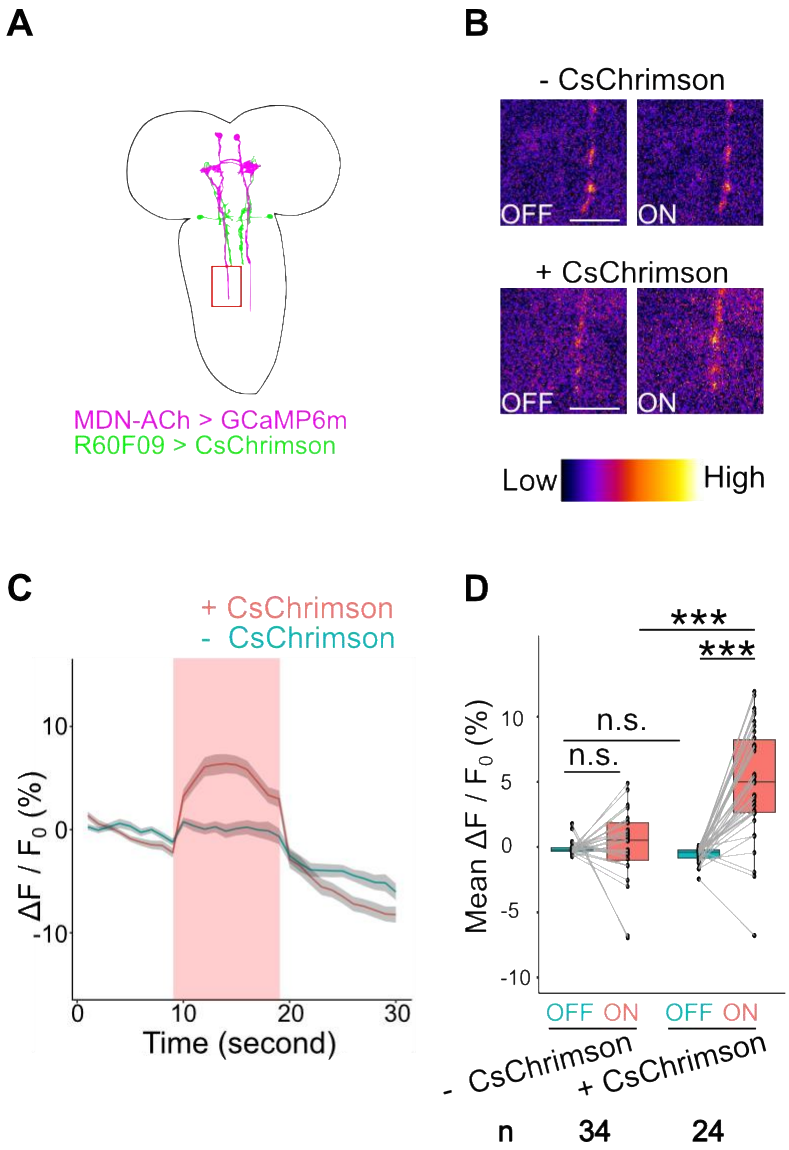


(A) A schematic view of AMBs and MDNs. The red box indicates the area observed in $Ca^{2+}$ imaging. (B) $Ca^{2+}$ imaging of MDNs upon optogenetic activation of AMBs in with (lower panels) or without CsChrimson (upper panels) conditions. Here are shown representative images of relative $Ca^{2+}$ levels 5 seconds before (OFF) and after (ON) light application. Scale bars, 10μm. (C) Time series of calcium responses in MDN axons upon optogenetic AMB activation. The red light was applied during the period indicated by the red band. Data are shown as the mean ± SEM. Genotypes: w;

UAS-GCaMP6m, tsh-GAL80/R60F09-LexA; R73F04-GAL4, Gad1-2A-GAL80/LexAop-CsChrimson (+CsChrimson); w; UAS-GCaMP6m, tsh-GAL80/+; R73F04-GAL4, Gad1-2A-GAL80/LexAop-CsChrimson (-CsChrimson). (D) Average of MDN $\Delta F/F_0$ values in 10 seconds before (OFF) or during (ON) optogenetic activation. In the boxplot, the width of the box represents the interquartile range. The whiskers extend to the data point that is less than 1.5 times the length of the box away from the box, and the dot represents the outlier. I assessed the statistical significance by Welch's t test with the Holm method. ***$p < 0.001$.

## Fig. 11. AMBs require MDNs to evoke backward waves.

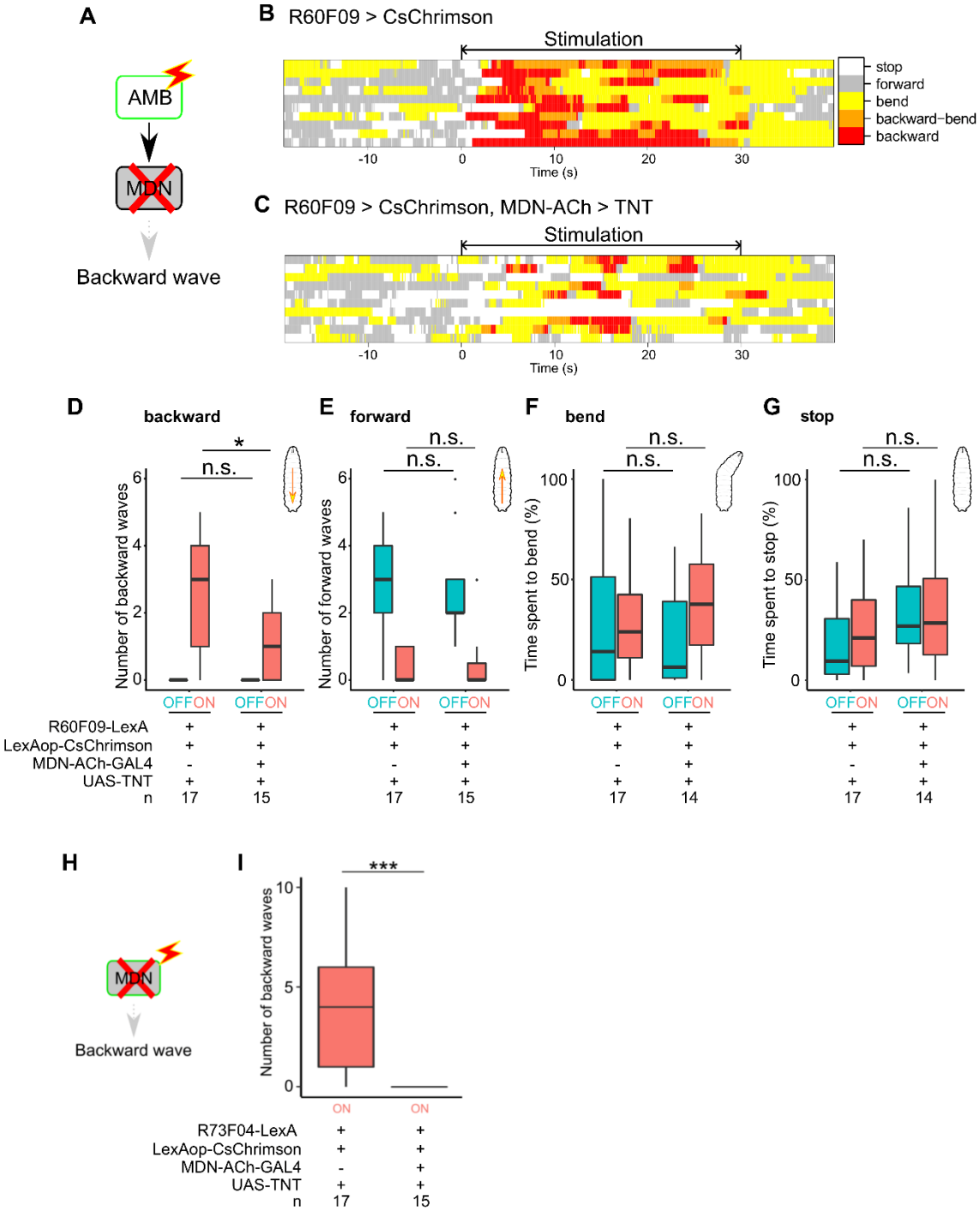


(A) A schematic view of optogenetic AMB activation with silencing MDNs. (B, C)

Representative behavior ethograms upon optogenetic stimulation of AMB neurons. An animal expressing CsChrimson in AMBs was subjected to optogenetic activation for 30 seconds. Behavior events are color-coded: forward movement (grey), stop (white), bending (yellow), bending with backward locomotion (orange) and backward locomotion (red). Representative data from 10 different animals are shown for each genotype. (D-G) The number of backward/forward waves or percentage of time spent in a behavioral mode in 10 seconds before (OFF) and during (ON) optogenetic AMB activation with CsChrimson while silencing MDNs. In the boxplot, the width of the box represents the interquartile range. The whiskers extend to the data point that is less than 1.5 times the length of the box away from the box, and the dot represents the outlier. (H-I) The number of backward waves in 30 seconds during optogenetic MDN activation with CsChrimson while silencing MDNs by TNT. I assessed the statistical significance by the Wilcoxon rank-sum test with the Holm method. *$p < 0.05$. ***$p < 0.001$.

**Fig. 12. Larval dead-end-induced backward waves are not mediated by either C3da, C4da or BO pathway and do not require either AMBs or MDNs.**

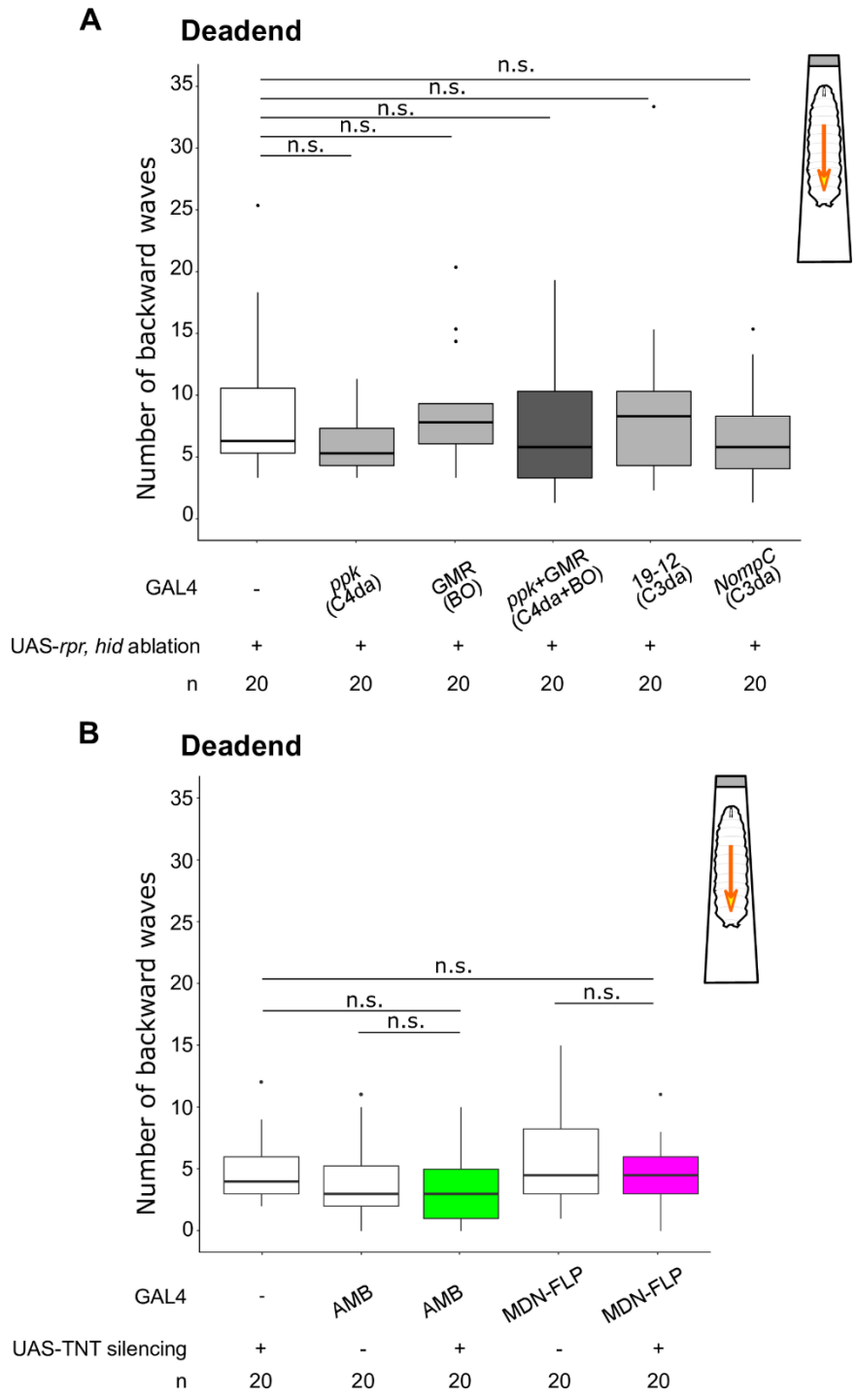

The number of backward waves evoked by the dead-end with the ablation of sensory neurons (A), or silencing AMBs or MDNs (B). The number of backward waves was counted for 1 min after an animal encounter the dead-end in the chamber. Genotypes are shown in Table. 1. In the boxplot, the width of the box represents the interquartile range. The whiskers extend to the data point that is less than 1.5 times the length of the box away from the box, and the dot represents the outlier. I assessed the statistical significance by the Wilcoxon rank-sum test with the Holm method.

**Fig. 13. Gentle touch-induced backward waves are mediated by C3da and require MDNs activity**

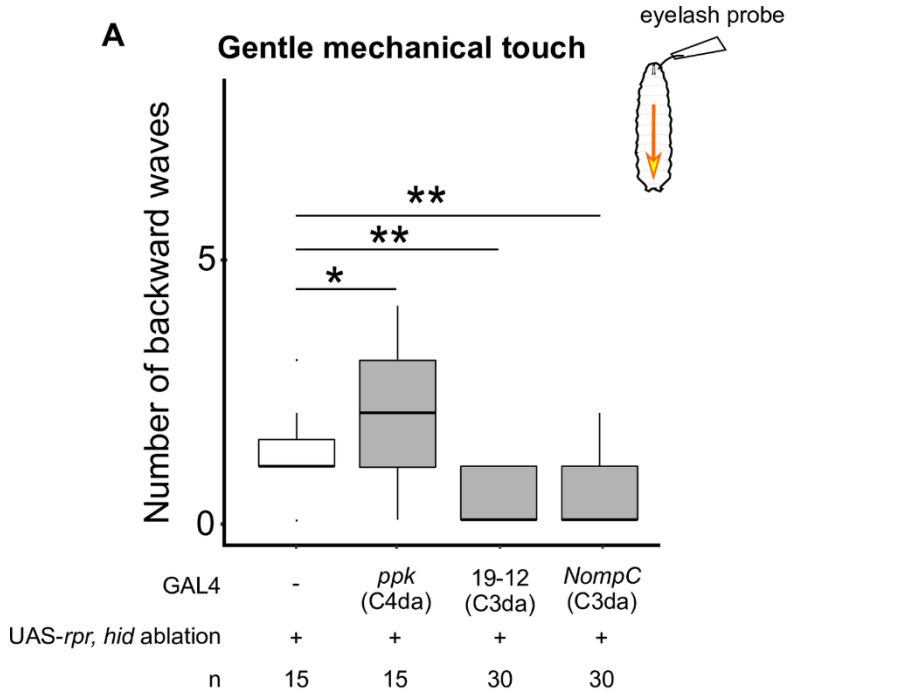


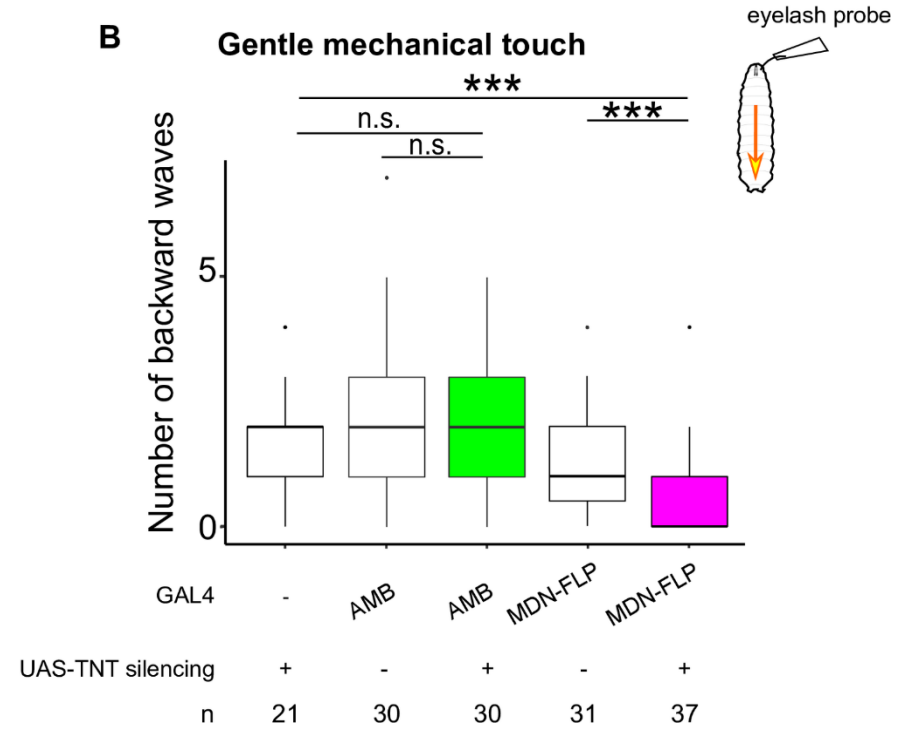

The number of backward waves in response to gentle touch with ablation of sensory neurons (A) or silencing AMBs or MDNs (B). The gentle touch was applied four times with 15 seconds intervals. Genotypes are shown in Table. 1. In the boxplot, the width of the box represents the interquartile range. The whiskers extend to the data point that is less than 1.5 times the length of the box away from the box, and the dot represents the outlier. I assessed the statistical significance by the Wilcoxon rank-sum test with the Holm method. * $p < 0.05$, ** $p < 0.01$, *** $p < 0.001$.

**Fig. 14. Blue light-induced backward waves are mediated by both the C4da-pathway and the BO pathway and require MDNs activity.**

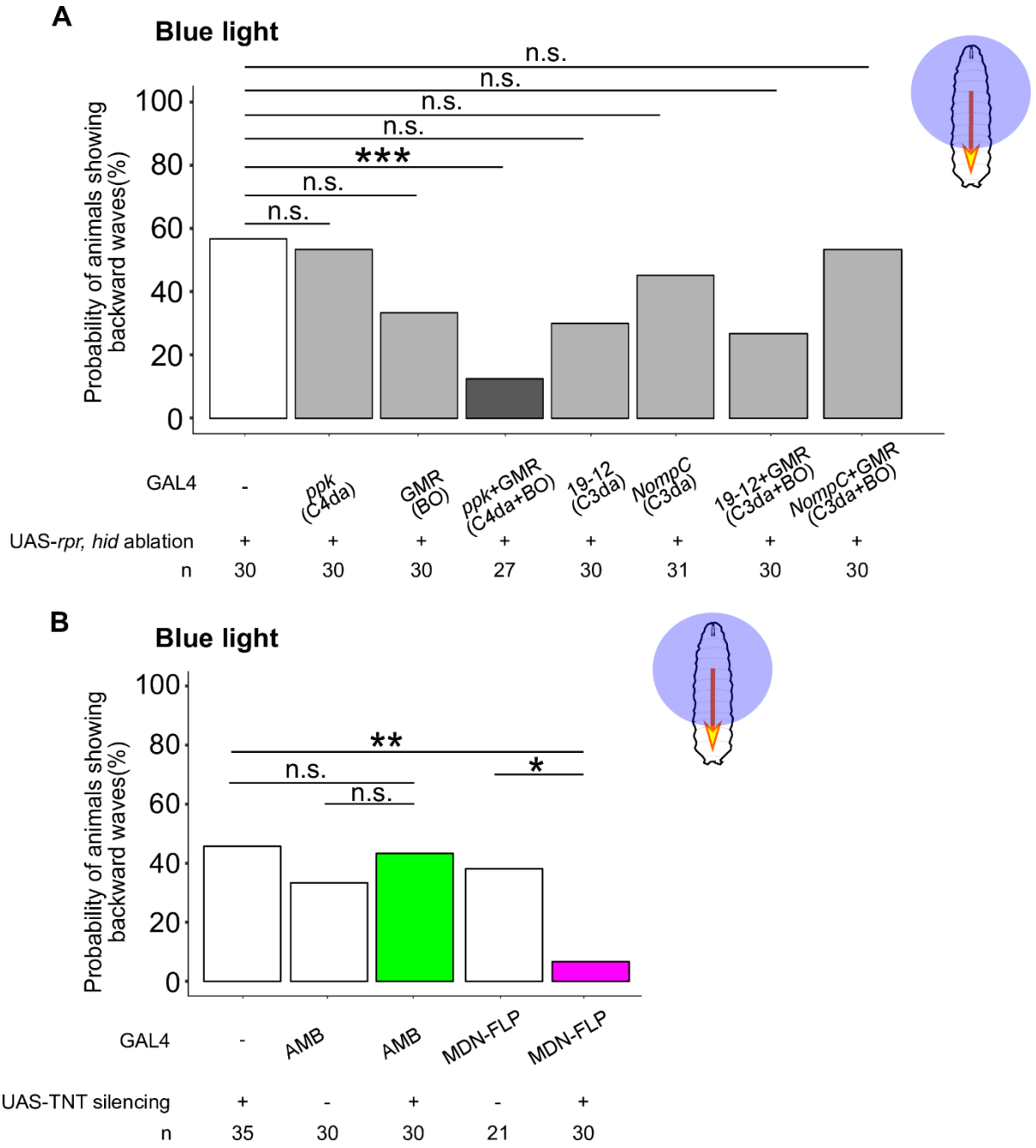


The probability of animals exhibiting backward waves upon blue light application with ablation of sensory neurons (A), or silencing AMBs or MDNs (B). The blue light was applied for 5 seconds. Genotypes are shown in Table. 1. I assessed the statistical significance by Fisher's exact test with the Holm method. * $p < 0.05$, ** $p < 0.01$.

**Fig. 15. The behavioral sequence induced by blue light irradiation is not largely affected by the silence of the AMB-MDN pathway.**

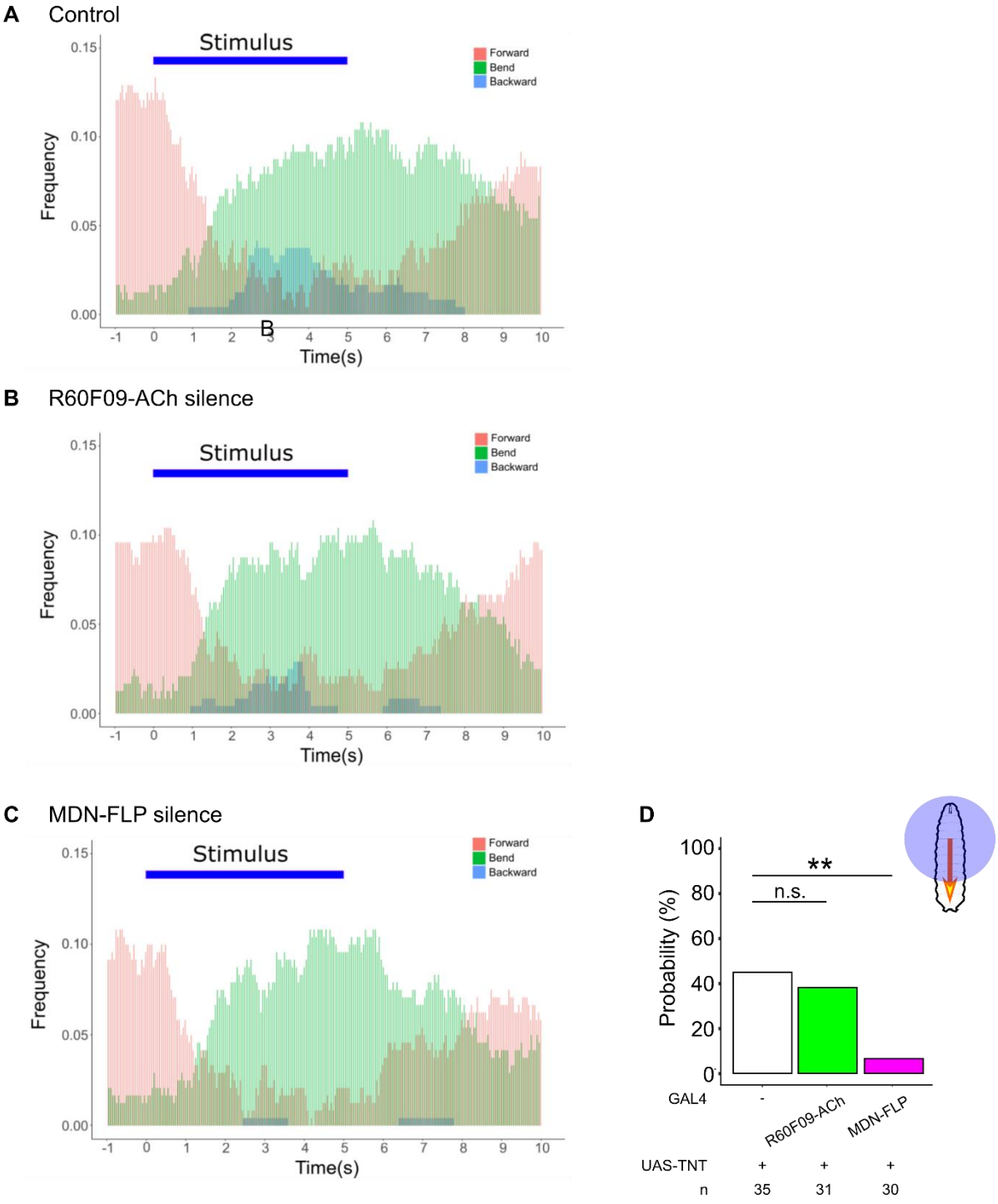

(A-C) The frequency of the behavior state was detected during the blue light irradiation experiment. Frequencies of forward run, bending, and backward locomotion are shown as red, green, and light blue, respectively. The stimulation timing is indicated by the blue lateral bar. (D) The probability of animals exhibiting backward waves upon blue light application. Genotypes are shown in Table. 1.

**Fig. 16. Neither AMBs nor MDNs has a direct connection with visual sensory neurons.**

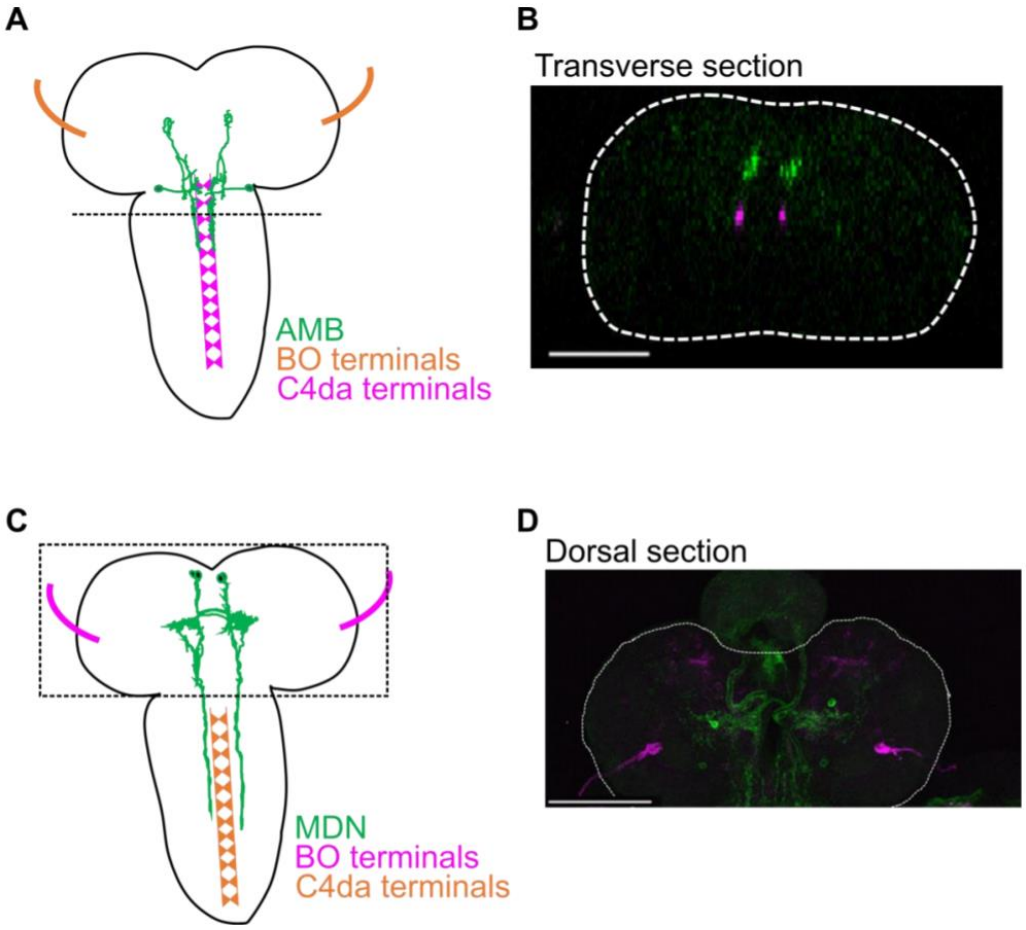


(A) A schematic view of AMBs and visual sensory neurons. The black dot line indicates the section indicated in the right picture. (B) Dual-labeling of C4da neurons and AMBs is shown in the transverse section. C4da neurons and AMBs are labeled with membrane-localized RFP and GFP, respectively. Scale bar, 50 μm. (C) A schematic view of MDNs and visual sensory neurons. The black dotted square indicates the section indicated in the right picture. (D) Dual-labeling of BO and MDNs is shown in the dorsal section. BO and MDNs are labeled with membrane-localized RFP and GFP, respectively. Scale bar, 100 μm.

**Fig. 17. C4da neurons require AMBs and MDNs to evoke backward locomotion.**

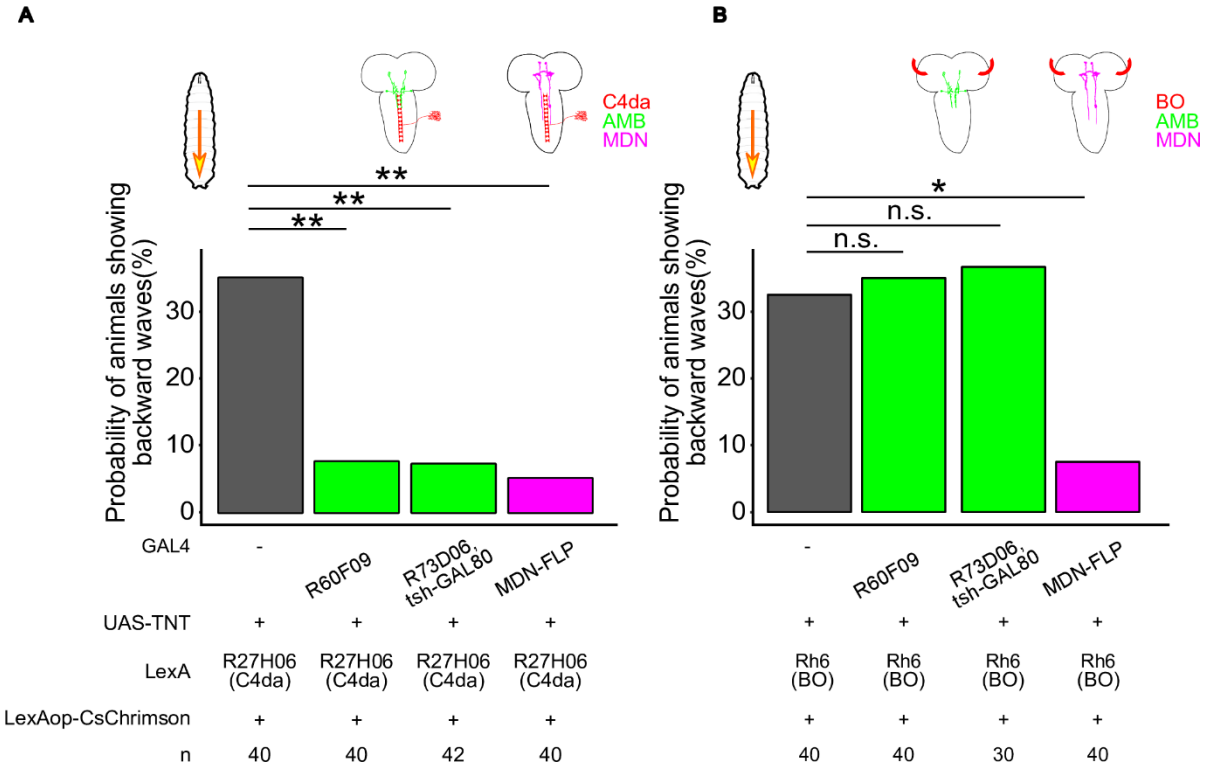


The probability of animals exhibiting backward waves during optogenetic activation of C4da neurons (A) or BO (B) for 30 seconds. I evaluated statistical significance by Fisher's exact test with the Holm method. *p < 0.05.

**Fig. 18. Optogenetic activation of C4da neurons evokes $Ca^{2+}$ responses in AMBs**

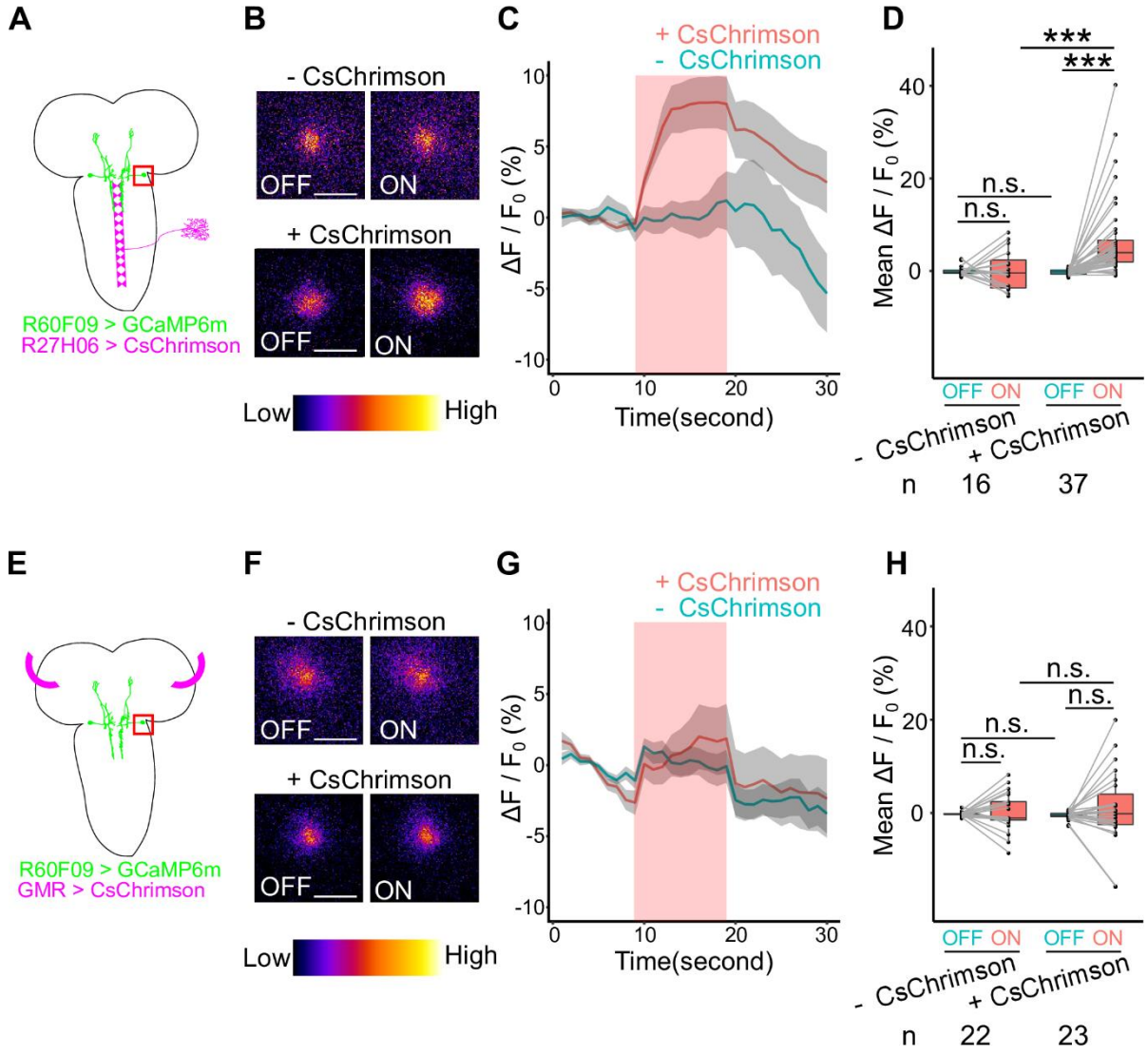


(A, E) Schematic views of $Ca^{2+}$ imaging on AMB's soma during optogenetic activation of sensory neurons. Genotypes: w; UAS-GCaMP6m, tsh-GAL80/R27H06-LexA; R60F09-GAL4/LexAop-CsChrimson (+CsChrimson); w; UAS-GCaMP6m, tsh-GAL80/+; R60F09-GAL4/LexAop-CsChrimson (-CsChrimson) (A-D); w; GMR-GAL4/R60F09-LexA; UAS-CsChrimson/LexAop-GCaMP6m (+CsChrimson); w; R60F09-LexA/+; UAS-CsChrimson/LexAop-GCaMP6m (-CsChrimson) (E-H). (B, F) $Ca^{2+}$ imaging of AMB neurons upon optogenetic activation of sensory neurons in +CsChrimson (lower panels) and -CsChrimson (upper panels) conditions. Here are shown

representative images of relative $Ca^{2+}$ levels 5 seconds before (OFF) and after (ON) light application. Scale bars, 10μm. (C, G) Time series of $Ca^{2+}$ responses in the soma of AMBs upon optogenetic activation of sensory neurons. I applied stimulation in the period indicated by the red band. Data are shown as the mean ± SEM. (D, H) Average of AMB $\Delta F/F_0$ values in 10 seconds before (OFF) or during (ON) optogenetic activation. In the boxplot, the width of the box represents the interquartile range. The whiskers extend to the data point that is less than 1.5 times the length of the box away from the box, and the dot represents the outlier. I assessed the statistical significance by paired t-test for paired samples and Welch's two-sample t-test for unpaired samples. ***$p < 0.001$.

**Fig. 19. Blue light irradiation evokes $Ca^{2+}$ responses in AMBs via C4da neurons.**

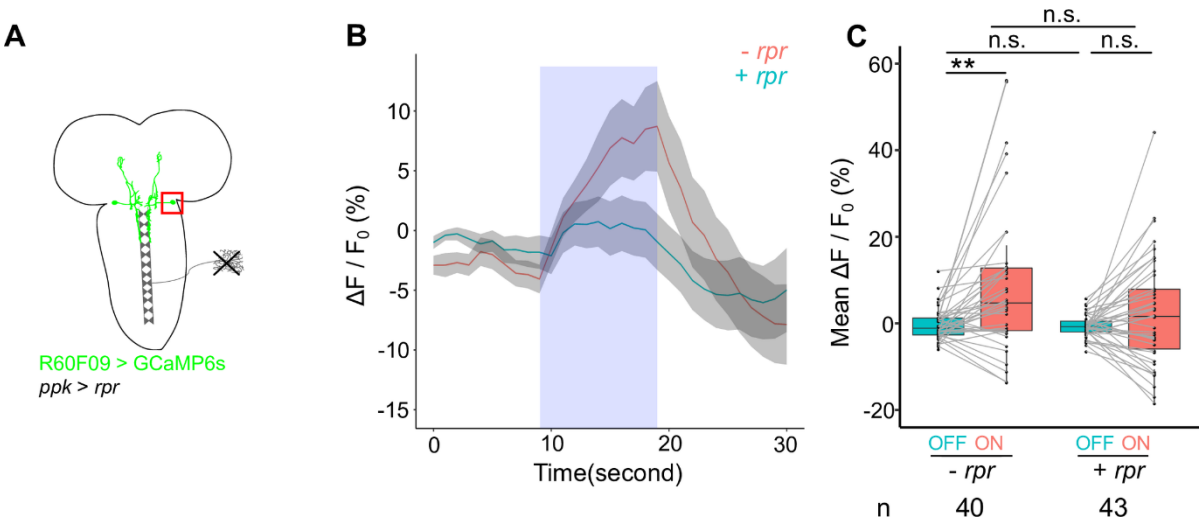


(A) A schematic view of $Ca^{2+}$ imaging on AMB's soma while ablating C4da neurons. Genotypes: UAS-rpr/+; R60F09-LexA, LexAop-GCaMP6s; ppk-GAL4/+ (+rpr); UAS-rpr/+; R60F09-LexA, LexAop-GCaMP6s; +/+ (-rpr). (B) Time series of $Ca^{2+}$ responses in the soma of AMBs upon blue light irradiation. I applied stimulation in the period indicated by the blue band. Data are shown as the mean ± SEM. (C) Average of AMB $\Delta F/F_0$ values in 5 seconds before (OFF) or last 5 seconds during (ON) optogenetic activation. In the boxplot, the width of the box represents the interquartile range. The whiskers extend to the data point that is less than 1.5 times the length of the box away from the box, and the dot represents the outlier. I assessed the statistical significance by paired t test for paired samples and Welch's two-sample t-test for unpaired samples. **$p < 0.01$.

**Fig. 20. Organization of the larval sensory systems to induce backward locomotion revealed in this study.**

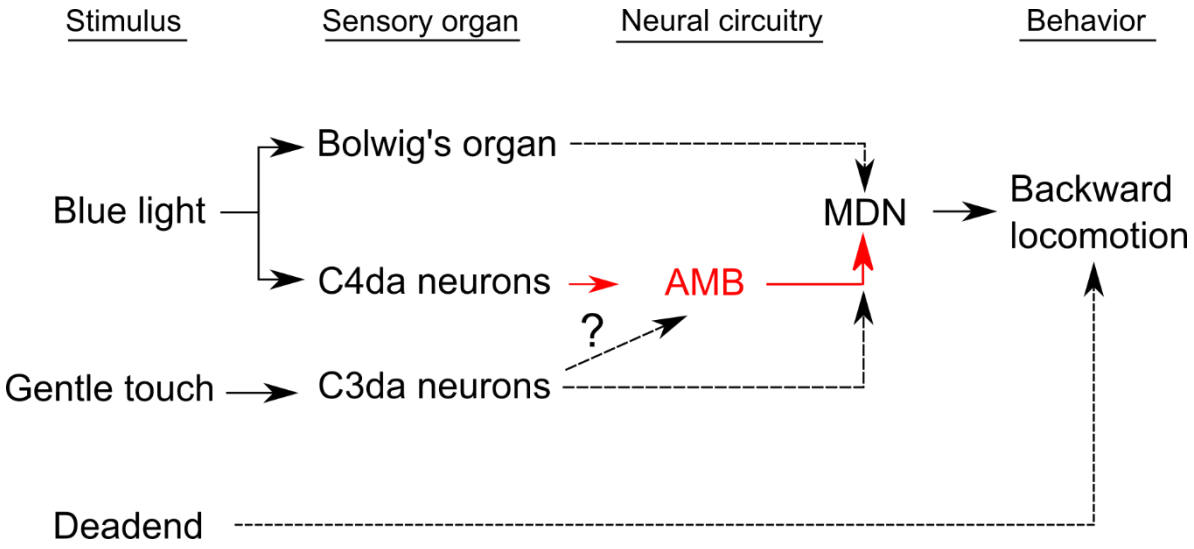


Black solid lines indicate the functional connections shown in the previous studies [6,29,30]. Red solid lines indicate the functional connections proven in this study. Black dashed lines indicate the functional connections implied in this study.

# Acknowledgments

I would like to thank C. Doe, D. Anderson, D. Allan, G. Miesenböck, H. Herranz, P. Soba, S. Berger-Müller, T. Suzuki, T. Lee, Bloomington Stock Center for reagents; FIM-Team for helping data analysis; S. Kondo for helpful advice in vector construction; the members of Emoto lab for critical comments and discussion (M. Tsuji and J. Yoshino for especially insightful suggestions; M. Sakai for experimental support); M. Miyahara and H. Itoh for technical assistance; J. Parrish for critical reading and comments. This work is supported by the Graduate Program for Leaders in Life Innovation (GPLLI) and Grant-in-Aid for JSPS Fellows to Natsuko Omamiuda-Ishikawa; MEXT Grants-in-Aid for Scientific Research on Innovative Areas "Dynamic regulation of brain function by Scrap & Build system" (KAKENHI 16H06456), JSPS (KAKENHI 16H02504), WPI-IRCN, AMED-CREST(JP18gm0610014), JST-CREST, the Strategic Research Program for Brain Sciences, Toray Foundation, Naito Foundation, Takeda Science Foundation, and Uehara Memorial Foundation to Kazuo Emoto. Finally, my sincere gratitude to my friends and family for their love, help, and support. E. Bergoglio, Y. Dairyo, E. Hasegawa, N. Utashiro, and A. Tezuka for their frequent support and creating a cordial working environment. I am thankful to F. Omamiuda for always being there for me as a friendly criticizer in discussion and a generous supporter in daily life. I am grateful to my sisters for giving me the experiences that have made me who I am. I cannot thank my parents enough for generous supports for whatever I want to do.

# References


1. Buford JA, Zernicke RF, Smith JL. Adaptive control for backward quadrupedal walking. I. Posture and hindlimb kinematics. J Neurophysiol. 1990;64: 745–755. doi:10.1152/jn.1990.64.3.745

2. Zelik KE, La Scaleia V, Ivanenko YP, Lacquaniti F. Can modular strategies simplify neural control of multidirectional human locomotion? J Neurophysiol. 2014;111: 1686–1702. doi:10.1152/jn.00776.2013

3. Islam SS, Zelenin P V. Modifications of Locomotor Pattern Underlying Escape Behavior in the Lamprey. J Neurophysiol. 2008;99: 297–307. doi:10.1152/jn.00903.2007

4. Liao JC, Fetcho JR. Shared versus specialized glycinergic spinal interneurons in axial motor circuits of larval zebrafish. J Neurosci. 2008;28: 12982–12992. doi:10.1523/JNEUROSCI.3330-08.2008

5. Chalfie M, Sulston JE, White JG, Southgate E, Thomson JN, Brenner S. The neural circuit for touch sensitivity in Caenorhabditis elegans. J Neurosci. 1985;5: 956–964. doi:3981252

6. Carreira-Rosario A, Zarin AA, Clark MQ, Manning L, Fetter RD, Cardona A, et al. MDN brain descending neurons coordinately activate backward and inhibit forward locomotion. Elife. 2018;7: e38554. doi:10.7554/eLife.38554

7. Kristan WB, Calabrese RL, Friesen WO. Neuronal control of leech behavior. Prog Neurobiol. 2005;76: 279–327. doi:10.1016/J.PNEUROBIO.2005.09.004

8. Edwards DH, Heitler WJ, Krasne FB. Fifty years of a command neuron: the neurobiology of escape behavior in the crayfish. Trends Neurosci. 1999;22: 153–161. doi:10.1016/S0166-2236(98)01340-X

9. Korn H, Faber DS. The Mauthner cell half a century later: A neurobiological model for decision-making? Neuron. 2005;47: 13–28. doi:10.1016/j.neuron.2005.05.019

10. Deliagina TG, Musienko PE, Zelenin P V. Nervous mechanisms of locomotion in different directions. Curr Opin Physiol. 2019;8: 7–13. doi:10.1016/j.cophys.2018.11.010

11. Caggiano V, Leiras R, Goñi-Erro H, Masini D, Bellardita C, Bouvier J, et al. Midbrain circuits that set locomotor speed and gait selection. Nature. 2018;553: 455–460. doi:10.1038/nature25448

12. Musienko PE, Zelenin P V., Lyalka VF, Gerasimenko YP, Orlovsky GN, Deliagina TG. Spinal and supraspinal control of the direction of stepping during locomotion. J Neurosci. 2012;32: 17442–17453. doi:10.1523/JNEUROSCI.3757-12.2012

13. Haspel G, O'Donovan MJ, Hart AC. Motoneurons dedicated to either forward or backward locomotion in the nematode Caenorhabditis elegans. J Neurosci. 2010;30: 11151–11156. doi:10.1523/JNEUROSCI.2244-10.2010

14. Lindsay TH, Thiele TR, Lockery SR. Optogenetic analysis of synaptic transmission in the central nervous system of the nematode Caenorhabditis elegans. Nat Commun. 2011;2. doi:10.1038/ncomms1304

15. Roberts WM, Augustine SB, Lawton KJ, Lindsay TH, Thiele TR, Izquierdo EJ, et al. A stochastic neuronal model predicts random search behaviors at multiple spatial scales in C. elegans. Elife. 2016;5. doi:10.7554/eLife.12572.001

16. Kupfermann I, Weiss KR. The command neuron concept. Behav Brain Sci. 1978;1: 3–10. doi:10.1017/S0140525X00059057

17. Wiersma CAG, Ikeda K. Interneurons commanding swimmeret movements in the crayfish, Procambarus clarki (girard). Comp Biochem Physiol Part A. 1964;12: 509–516.

doi:10.1016/0010-406x(64)90153-7

18. Kaplan HS, Nichols ALA, Zimmer M. Sensorimotor integration in Caenorhabditis elegans: A reappraisal towards dynamic and distributed computations. Philos Trans R Soc B Biol Sci. 2018;373. doi:10.1098/rstb.2017.0371

19. Gray JM, Hill JJ, Bargmann CI. A circuit for navigation in Caenorhabditis elegans. Proc Natl Acad Sci U S A. 2005;102: 3184–3191. doi:10.1073/pnas.0409009101

20. Iyengar BG, Chou CJ, Sharma A, Atwood HL. Modular neuropile organization in the Drosophila larval brain facilitates identification and mapping of central neurons. J Comp Neurol. 2006;499: 583–602. doi:10.1002/cne.21133

21. Pfeiffer BD, Ngo T-TB, Hibbard KL, Murphy C, Jenett A, Truman JW, et al. Refinement of tools for targeted gene expression in Drosophila. Genetics. 2010;186: 735–755. doi:10.1534/genetics.110.119917

22. Jenett A, Rubin GM, Ngo TTB, Shepherd D, Murphy C, Dionne H, et al. A GAL4-Driver Line Resource for Drosophila Neurobiology. Cell Rep. 2012;2: 991–1001. doi:10.1016/j.celrep.2012.09.011

23. Kohsaka H, Zwart MF, Fushiki A, Fetter RD, Truman JW, Cardona A, et al. Regulation of forward and backward locomotion through intersegmental feedback circuits in Drosophila larvae. Nat Commun. 2019;10. doi:10.1038/s41467-019-10695-y

24. Bidaye SS, Machacek C, Wu Y, Dickson BJ. Neuronal Control of Drosophila Walking Direction. Science (80- ). 2014;344: 97–101. doi:10.1126/science.1249964

25. Sen R, Wang K, Dickson BJ. TwoLumps Ascending Neurons Mediate Touch-Evoked Reversal of Walking Direction in Drosophila. Curr Biol. 2019;29: 4337-4344.e5. doi:10.1016/j.cub.2019.11.004

26. Sen R, Wu M, Branson K, Robie A, Rubin GM, Dickson BJ. Moonwalker Descending Neurons Mediate Visually Evoked Retreat in Drosophila. Curr Biol. 2017;27: 766–771. doi:10.1016/j.cub.2017.02.008

27. Takagi S, Cocanougher BT, Niki S, Miyamoto D, Kohsaka H, Kazama H, et al. Divergent Connectivity of Homologous Command-like Neurons Mediates Segment-Specific Touch Responses in Drosophila. Neuron. 2017;96: 1373-1387.e6. doi:10.1016/j.neuron.2017.10.030

28. Wu M, Nern A, Ryan Williamson W, Morimoto MM, Reiser MB, Card GM, et al. Visual projection neurons in the Drosophila lobula link feature detection to distinct behavioral programs. Elife. 2016;5. doi:10.7554/eLife.21022

29. Xiang Y, Yuan Q, Vogt N, Looger LL, Jan LY, Jan YN. Light-avoidance-mediating photoreceptors tile the Drosophila larval body wall. Nature. 2010;468: 921–926. doi:10.1038/nature09576

30. Yan Z, Zhang W, He Y, Gorczyca D, Xiang Y, Cheng LE, et al. Drosophila NOMPC is a mechanotransduction channel subunit for gentle-touch sensation. Nature. 2012;493: 221–225. doi:10.1038/nature11685

31. Kim SE, Coste B, Chadha A, Cook B, Patapoutian A. The role of Drosophila Piezo in mechanical nociception. Nature. 2012;483: 209–212. doi:10.1038/nature10801

32. Salcedo E, Huber A, Henrich S, Chadwell L V, Chou WH, Paulsen R, et al. Blue- and green-absorbing visual pigments of Drosophila: ectopic expression and physiological characterization of the R8 photoreceptor cell-specific Rh5 and Rh6 rhodopsins. J Neurosci. 1999;19: 10716–10726. doi:10.1523/JNEUROSCI.19-24-10716.1999

33. Sprecher SG, Pichaud F, Desplan C. Adult and larval photoreceptors use different

mechanisms to specify the same Rhodopsin fates. Genes Dev. 2007;21: 2182–2195. doi:10.1101/gad.1565407

34. Guntur AR, Gu P, Takle K, Chen J, Xiang Y, Yang CH. Drosophila TRPA1 isoforms detect UV light via photochemical production of H2O2. Proc Natl Acad Sci U S A. 2015;112: E5753–E5761. doi:10.1073/pnas.1514862112

35. Yoshino J, Morikawa RK, Hasegawa E, Emoto K. Neural Circuitry that Evokes Escape Behavior upon Activation of Nociceptive Sensory Neurons in Drosophila Larvae. Curr Biol. 2017;27: 2499-2504.e3. doi:10.1016/J.CUB.2017.06.068

36. Burgos A, Honjo K, Ohyama T, Qian CS, Shin GJ, Gohl DM, et al. Nociceptive interneurons control modular motor pathways to promote escape behavior in Drosophila. Elife. 2018;7: e26016. doi:10.7554/eLife.26016

37. Ohyama T, Schneider-Mizell CM, Fetter RD, Aleman JV, Franconville R, Rivera-Alba M, et al. A multilevel multimodal circuit enhances action selection in Drosophila. Nature. 2015;520: 633–639. doi:10.1038/nature14297

38. Hu C, Petersen M, Hoyer N, Spitzweck B, Tenedini F, Wang D, et al. Sensory integration and neuromodulatory feedback facilitate Drosophila mechanonociceptive behavior. Nat Neurosci. 2017;20: 1085–1095. doi:10.1038/nn.4580

39. Larderet I, Fritsch PM, Gendre N, Neagu-Maier GL, Fetter RD, Schneider-Mizell CM, et al. Organization of the Drosophila larval visual circuit. Elife. 2017;6: e28387. doi:10.7554/eLife.28387

40. Schneider-Mizell CM, Gerhard S, Longair M, Kazimiers T, Li F, Zwart MF, et al.Quantitative neuroanatomy for connectomics in Drosophila. Elife. 2016;5: e12059. doi:10.7554/eLife.12059

41. Maimon G, Straw AD, Dickinson MH. A Simple Vision-Based Algorithm for Decision Making in Flying Drosophila. Curr Biol. 2008;18: 464–470. doi:10.1016/j.cub.2008.02.054

42. Mazzoni EO, Desplan C, Blau J. Circadian Pacemaker Neurons Transmit and Modulate Visual Information to Control a Rapid Behavioral Response. Neuron. 2005;45: 293–300. doi:10.1016/j.neuron.2004.12.038

43. McGuire SE, Le PT, Osborn AJ, Matsumoto K, Davis RL. Spatiotemporal rescue of memory dysfunction in Drosophila. Sci York, NY). 2003;302: 1765–1768. doi:10.1126/science.1089035

44. Park J, Kondo S, Tanimoto H, Kohsaka H, Nose A. Data-driven analysis of motor activity implicates 5-HT2A neurons in backward locomotion of larval Drosophila. Sci Rep. 2018;8: 10307. doi:10.1038/s41598-018-28680-8

45. Kondo S, Ueda R, Phillis RW, Johnson-Schlitz DM, Benz WK. Highly improved gene targeting by germline-specific Cas9 expression in Drosophila. Genetics. 2013;195: 715–721. doi:10.1534/genetics.113.156737

46. Klapoetke NC, Murata Y, Kim SS, Pulver SR, Birdsey-Benson A, Cho YK, et al. Independent optical excitation of distinct neural populations. Nat Methods. 2014;11: 338–346. doi:10.1038/nmeth.2836

47. Röder L, Vola C, Kerridge S. The role of the teashirt gene in trunk segmental identity in Drosophila. Development. 1992;115: 1017–1033.

48. Fasano L, Röder L, Coré N, Alexandre E, Vola C, Jacq B, et al. The gene teashirt is required for the development of Drosophila embryonic trunk segments and encodes a protein with widely spaced zinc finger motifs. Cell. 1991;64: 63–79. doi:10.1016/0092-8674(91)90209-H

49. Mahr A, Aberle H. The expression pattern of the Drosophila vesicular glutamate transporter: A marker protein for motoneurons and glutamatergic centers in the brain. Gene Expr Patterns. 2006;6: 299–309. doi:10.1016/j.modgep.2005.07.006

50. Chalfie M, Hart AC, Rankin CH, Goodman MB. Assaying mechanosensation. WormBook. 2013 [cited 12 Dec 2019]. doi:10.1895/wormbook.1.172.1

51. Risse B, Berh D, Otto N, Klämbt C, Jiang X. FIMTrack: An open source tracking and locomotion analysis software for small animals. Poisot T, editor. PLOS Comput Biol. 2017;13: e1005530. doi:10.1371/journal.pcbi.1005530

52. Feng Y, Ueda A, Wu C. A modified minimal hemolymph-like solution, HL3.1, for physiological recordings at the neuromuscular junctions of normal and mutant Drosophila larvae. J Neurogenet. 2004;18: 377–402. doi:10.1080/01677060490894522

53. Gordon MD, Scott K. Motor Control in a Drosophila Taste Circuit. Neuron. 2009;61: 373–384. doi:10.1016/J.NEURON.2008.12.033

54. Bohm RA, Welch WP, Goodnight LK, Cox LW, Henry LG, Gunter TC, et al. A genetic mosaic approach for neural circuit mapping in Drosophila. Proc Natl Acad Sci. 2010;107: 16378–16383. doi:10.1073/pnas.1004669107

55. Nicolai LJJ, Ramaekers A, Raemaekers T, Drozdzecki A, Mauss AS, Yan J, et al. Genetically encoded dendritic marker sheds light on neuronal connectivity in Drosophila. Proc Natl Acad Sci. 2010;107: 20553–20558. doi:10.1073/pnas.1010198107

56. Fouquet W, Owald D, Wichmann C, Mertel S, Depner H, Dyba M, et al. Maturation of active zone assembly by Drosophila Bruchpilot. J Cell Biol. 2009;186: 129–145. doi:10.1083/jcb.200812150

57. Kolodziejczyk A, Sun X, Meinertzhagen IA, Nässel DR. Glutamate, GABA and

Acetylcholine Signaling Components in the Lamina of the Drosophila Visual System. Callaerts P, editor. PLoS One. 2008;3: e2110. doi:10.1371/journal.pone.0002110

58. Feinberg EH, VanHoven MK, Bendesky A, Wang G, Fetter RD, Shen K, et al. GFP Reconstitution Across Synaptic Partners (GRASP) Defines Cell Contacts and Synapses in Living Nervous Systems. Neuron. 2008;57: 353–363. doi:10.1016/j.neuron.2007.11.030

59. Shearin HK, Quinn CD, Mackin RD, Macdonald IS, Stowers RS. t-GRASP, a targeted GRASP for assessing neuronal connectivity. J Neurosci Methods. 2018;306: 94–102. doi:10.1016/j.jneumeth.2018.05.014

60. Sweeney ST, Broadie K, Keane J, Niemann H, O'Kane CJ. Targeted expression of tetanus toxin light chain in Drosophila specifically eliminates synaptic transmission and causes behavioral defects. Neuron. 1995;14: 341–351.

61. White K, Tahaoglu E, Steller H. Cell killing by the Drosophila gene reaper. Science. 1996;271: 805–807. doi:10.1126/SCIENCE.271.5250.805

62. White K, Grether ME, Abrams JM, Young L, Farrell K, Steller H. Genetic control of programmed cell death in Drosophila. Science. 1994;264: 677–683.

63. Abbott MK, Lengyel JA. Embryonic head involution and rotation of male terminalia require the Drosophila locus head involution defective. Genetics. 1991;129: 783–789.

64. Berger-Müller S, Sugie A, Takahashi F, Tavosanis G, Hakeda-Suzuki S, Suzuki T. Assessing the Role of Cell-Surface Molecules in Central Synaptogenesis in the Drosophila Visual System. Chien C-T, editor. PLoS One. 2013;8: e83732. doi:10.1371/journal.pone.0083732

65. Hughes CL, Thomas JB. A sensory feedback circuit coordinates muscle activity in

Drosophila. Mol Cell Neurosci. 2007;35: 383–396. doi:10.1016/j.mcn.2007.04.001

66. Vaadia RD, Li W, Voleti V, Singhania A, Hillman EMCC, Grueber WB. Characterization of Proprioceptive System Dynamics in Behaving Drosophila Larvae Using High-Speed Volumetric Microscopy. 2019;29: 935-944.e4. doi:10.1016/j.cub.2019.01.060

67. Vogelstein JT, Park Y, Ohyama T, Kerr RA, Truman JW, Priebe CE, et al. Discovery of brainwide neural-behavioral maps via multiscale unsupervised structure learning. Science. 2014;344: 386–92. doi:10.1126/science.1250298

68. Terada S-I, Matsubara D, Onodera K, Matsuzaki M, Uemura T, Usui T. Neuronal processing of noxious thermal stimuli mediated by dendritic Ca2+ influx in Drosophila somatosensory neurons. Elife. 2016;5:e12959. doi:10.7554/eLife.12959

69. Machens CK, Romo R, Brody CD. Flexible Control of Mutual Inhibition: A Neural Model of Two-Interval Discrimination. Science (80- ). 2005;307: 1121–1124. doi:10.1126/science.1104171

70. Jovanic T, Schneider-Mizell CM, Shao M, Masson JB, Denisov G, Fetter RD, et al. Competitive Disinhibition Mediates Behavioral Choice and Sequences in Drosophila. Cell. 2016;167: 858-870.e19. doi:10.1016/j.cell.2016.09.009

71. Hart AC, Kass J, Shapiro JE, Kaplan JM. Distinct signaling pathways mediate touch and osmosensory responses in a polymodal sensory neuron. J Neurosci. 1999;19: 1952–1958. doi:10.1523/jneurosci.19-06-01952.1999

72. Hilliard MA, Apicella AJ, Kerr R, Suzuki H, Bazzicalupo P, Schafer WR. In vivo imaging of C. elegans ASH neurons: Cellular response and adaptation to chemical repellents. EMBO J. 2005;24: 63–72. doi:10.1038/sj.emboj.7600493

73. Sambongi Y, Nagae T, Liu Y, Yoshimizu T, Takeda K, Wada Y, et al. Sensing of cadmium and copper ions by externally exposed ADL, ASE, and ASH neurons elicits avoidance response in Caenorhabditis elegans. Neuroreport. 1999;10: 753–757. doi:10.1097/00001756-199903170-00017

74. Li W, Kang L, Piggott BJ, Feng Z, Xu XZS. The neural circuits and sensory channels mediating harsh touch sensation in Caenorhabditis elegans. Nat Commun. 2011;2. doi:10.1038/ncomms1308

75. Goodman MB. Mechanosensation. WormBook. 2006 [cited 12 Dec 2019]. doi:10.1895/wormbook.1.62.1

76. Williams DW, Shepherd D. Persistent larval sensory neurons in adult Drosophila melanogaster. J Neurobiol. 1999;39: 275–86.

77. Hu Y, Wang Z, Liu T, Zhang W. Piezo-like gene regulates locomotion in Drosophila larvae. Cell reports. 2019;26(6):1369-1377. doi: 10.1016/j.celrep.2019.01.055